



**HAL**  
open science

**Linearly implicit time integration scheme of Lagrangian systems via quadratization of a nonlinear kinetic energy. Application to a rotating flexible piano hammer shank**

Guillaume Castera, Juliette Chabassier

► **To cite this version:**

Guillaume Castera, Juliette Chabassier. Linearly implicit time integration scheme of Lagrangian systems via quadratization of a nonlinear kinetic energy. Application to a rotating flexible piano hammer shank. ESAIM: Mathematical Modelling and Numerical Analysis, 2024, 58 (5), pp.1881-1905. 10.1051/m2an/2024049 . hal-04731901

**HAL Id: hal-04731901**

**<https://hal.science/hal-04731901v1>**

Submitted on 11 Oct 2024

**HAL** is a multi-disciplinary open access archive for the deposit and dissemination of scientific research documents, whether they are published or not. The documents may come from teaching and research institutions in France or abroad, or from public or private research centers.

L'archive ouverte pluridisciplinaire **HAL**, est destinée au dépôt et à la diffusion de documents scientifiques de niveau recherche, publiés ou non, émanant des établissements d'enseignement et de recherche français ou étrangers, des laboratoires publics ou privés.

# LINEARLY IMPLICIT TIME INTEGRATION SCHEME OF LAGRANGIAN SYSTEMS VIA QUADRATIZATION OF A NONLINEAR KINETIC ENERGY. APPLICATION TO A ROTATING FLEXIBLE PIANO HAMMER SHANK

GUILLAUME CASTERA\* AND JULIETTE CHABASSIER

**Abstract.** This paper presents a general and practical approach for nonlinear energy quadratization based on the Euler–Lagrange formulation of the physical equations. A Scalar Auxiliary Variable -like method based on a phase formulation of the equations is applied. The proposed scheme is linearly implicit, reproduces a discrete equivalent of the power balance. It is applied to a rotating and flexible piano hammer shank. An efficient solving strategy leads to a quasi explicit algorithm which shows quadratic space/time convergence.

**Mathematics Subject Classification.** 00A71, 00A65, 35L05, 37K58, 70K25, 74H15, 65M06, 65M60, 37M15, 37N15.

Received August 17, 2023. Accepted June 13, 2024.

## 1. INTRODUCTION

Nonlinear equations are quite frequently encountered in many application domains like acoustics, fluid and solid state, optics, quantum, and others. We consider in this work an Euler–Lagrange system of equations, which can also be described entirely from the knowledge of a Hamiltonian function. These systems have power balance identities that can be exploited to perform the mathematical analysis of the equations.

Such a property is also very useful for numerical computation as ensuring the preservation of a discrete analog of the power balance identity, at least in simple cases, allows to derive *a-posteriori* stability estimates and convergence results of the time integration scheme [10, 21]. These estimates can especially be used to couple multiple systems even if each one of them has a different integration strategy.

Among all the nonlinear terms encountered in physics, we can distinguish the potential nonlinear terms depending only of the unknown field, and the kinetic ones that usually depend on the unknown field and its time derivatives.

A widely spread strategy to solve nonlinear Hamiltonian equations with power balanced methods is the use of Discrete Gradients. In [17, 27] such schemes are used in space dimensions 2 and 3. Allen–Cahn and Cahn–Hilliard equations are discretized in [28] where convergence proofs are also given. Non-linear elasticity is considered in [16], and in [2, 12], a Discrete Gradient approach is used to tackle contact terms in musical acoustics. In [11] such schemes are used for the 1D non-linear piano string, and [9] a discrete gradient scheme is applied to a rotating flexible hammer shank, which has both potential and kinetic nonlinear energies.

---

*Keywords and phrases.* Energy quadratization, Scalar Auxiliary Variable, Scalar Lagrangian Quadratization, flexible piano hammer shank.

MAKUTU Research Team, Inria Bordeaux University, Laboratoire de Mathématiques et leurs Applications de Pau, 200 avenue de la vieille Tour, 33400 Talence, France.

\*Corresponding author: [guillaume.castera@inria.fr](mailto:guillaume.castera@inria.fr)

© The authors. Published by EDP Sciences, SMAI 2024

The discrete gradient schemes have the major drawback of leading to implicit non-linear schemes that must be solved with iterative techniques. It requires to choose a convergence threshold, and induces a consequent number of iterations depending on how “hard” the nonlinear term is. The computation cost is often very high and unpredictable, as well as the implementation effort.

Recently appeared strategies guarantee a discrete power balance identity while increasing efficiency with linearly implicit numerical schemes. The so-called Invariant Energy Quadratzation (IEQ) schemes were introduced in [35, 36] in the context of phase-fields models. The so-called Scalar Auxiliary Variable (SAV) schemes introduced in [29] and all its variants [25, 26] were applied to gradient flows, but also for incompressible Navier–Stokes [23], Sine-Gordon equation [19], or general Hamiltonian equations [3, 20, 22]. These techniques were applied recently to the geometrically exact piano string in [13–15].

Although the literature is very rich and creative, the quadratized nonlinear terms are always of potential type. To the best of our knowledge, there is no method that could allow to use IEQ or SAV-like methods to solve kinetic nonlinear systems.

In the first part of this paper, we present a quadratization process based on the weak Euler–Lagrange equations for any kind of nonlinear energy, potential and kinetic. A time discretization strategy based on a phase formulation of the equations is proposed and applied in the second part to the rotating and flexible piano hammer shank described in [9] hitting first a rigid wall, then a vibrating string. The desire to write an efficient and precise integration method to compute the vibrations of the piano hammer shank comes from the past studies [9, 18, 33] which raise the question of the influence of the pianistic touch on the sound. The authors point out that the bending of the shank could depend of the input of the pianist and then create a scuffing motion of the hammer head on the string depending on the touch and therefore influencing the sound. Simulation of these subtle phenomena requires precise, stable and efficient numerical methods. The scheme proposed in this work ensures unconditional power balance preservation, and shows quadratic space/time convergence. A solving strategy leads to a quasi explicit algorithm. The presented application cases are of interest for a realistic modeling of the piano, but their nonlinear kinetic energy is not distributed over space. Hence, they do not illustrate all the possibilities offered by the algorithm proposed in the first section, which could be tested in a further work on more intricate systems of equations.

## 2. SCALAR LAGRANGIAN QUADRATIZATION TECHNIQUE FOR NONLINEAR EQUATIONS

Let  $\Omega \subset \mathbb{R}^N$  be a bounded domain. Let us consider a physical system described by some vectorial unknown  $q \equiv q(x, t)$ , for  $x \in \Omega$  and  $t \in [0, T]$ , expected to belong to  $C^1([0, T], V) \cap C^2([0, T], H)$ , where  $H$  is a Hilbert space equipped with a norm  $\|\cdot\|_H = \sqrt{(\cdot, \cdot)_H}$  on  $\Omega$ , typically  $L^2(\Omega)$ , and  $V \subset H$  another Hilbert space equipped with a norm induced by a symmetrical and invertible operator  $A_{11} : V \rightarrow H : \|\cdot\|_V = (A_{11}\cdot, \cdot)_H$ , and possibly accounting for some essential boundary conditions, typically  $H_0^1(\Omega)$  which is induced by the Laplace operator. Let  $\mathcal{L} : V \times V \rightarrow \mathbb{R}$  be the Lagrangian of the system and  $\mathcal{H} : V \times V \rightarrow \mathbb{R}$  the function defined by

$$\forall (q_1, q_2) \in V^2, \quad \mathcal{H}(q_1, q_2) = \frac{\partial \mathcal{L}}{\partial q_2}(q_1, q_2)(q_2) - \mathcal{L}(q_1, q_2) = \mathcal{I}(q_1, q_2) - \mathcal{L}(q_1, q_2), \tag{1}$$

with

$$\forall (q_1, q_2) \in V^2, \quad \mathcal{I}(q_1, q_2) = \frac{\partial \mathcal{L}}{\partial q_2}(q_1, q_2)(q_2), \tag{2}$$

where the directional derivatives of the Lagrangian function are such that for all  $(q_1, q_2) \in V^2$ ,

$$\begin{aligned} \frac{\partial \mathcal{L}}{\partial q_1}(q_1, q_2) : \left. \begin{array}{l} V \longrightarrow \mathbb{R} \\ q^* \longmapsto \lim_{h \rightarrow 0} \frac{\mathcal{L}(q_1 + hq^*, q_2) - \mathcal{L}(q_1, q_2)}{h} \end{array} \right|, & \quad \frac{\partial \mathcal{L}}{\partial q_2}(q_1, q_2) : \left. \begin{array}{l} V \longrightarrow \mathbb{R} \\ q^* \longmapsto \lim_{h \rightarrow 0} \frac{\mathcal{L}(q_1, q_2 + hq^*) - \mathcal{L}(q_1, q_2)}{h} \end{array} \right|, & \tag{3} \\ \frac{\partial^2 \mathcal{L}}{\partial q_1 \partial q_2}(q_1, q_2) : \left. \begin{array}{l} V \longrightarrow (V \longrightarrow \mathbb{R}) \\ q^* \longmapsto \lim_{h \rightarrow 0} \frac{\frac{\partial \mathcal{L}}{\partial q_2}(q_1 + hq^*, q_2) - \frac{\partial \mathcal{L}}{\partial q_2}(q_1, q_2)}{h} \end{array} \right|. & \end{aligned}$$

Note that by definition these derivatives are linear with respect to the argument  $q^*$ .



**Remark 2.3.** In this formalism, we implicitly assume that  $A_{11}$  is the operator that requires the most regularity, and whose natural space is  $V$ . Indeed, the operators  $A_{ij}$  often found in physics are such that  $A_{11}$  acts like a Laplace operator, and  $A_{22}$  is a simple constant weighting term. The bijective nature of  $A_{11} : V \rightarrow H$  is usually respected for suitable boundary conditions like Dirichlet, using classical elliptic theory results. Any model that would not satisfy these assumptions would necessitate another functional framework.

This allows to define a linear operator  $\widetilde{\mathcal{L}}$  such that for all  $(q_1, q_2, q_3, q_4) \in V \times V \times V \times H$  and all  $q^* \in V$

$$\widetilde{\mathcal{L}}(q_1, q_2, q_3, q_4, q^*) = \frac{\partial^2 \mathcal{L}_{\text{LIN}}}{\partial q_2^2}(q_1, q_2)(q_4)(q^*) + \frac{\partial^2 \mathcal{L}_{\text{LIN}}}{\partial q_1 \partial q_2}(q_1, q_2)(q_3)(q^*) - \frac{\partial \mathcal{L}_{\text{LIN}}}{\partial q_1}(q_1, q_2)(q^*) \tag{13}$$

$$= (A_{22}q_4, q^*)_H + (A_{12}q_3, q^*)_H - (A_{12}q_2, q^*)_H + (A_{11}q_1, q^*)_H + (V_1, q^*)_H, \tag{14}$$

and such that for the specific case  $q_1 = q, q_2 = q_3 = \dot{q}$  and  $q_4 = \ddot{q}$  we have

$$\widetilde{\mathcal{L}}(q, \dot{q}, \dot{q}, \ddot{q}, q^*) = (A_{22}\ddot{q}, q^*)_H + (A_{11}q, q^*)_H + (V_1, q^*)_H. \tag{15}$$

This leads to the definition of an other linear operator  $\mathcal{L}$  such that for all  $(q_1, q_2) \in V \times H$  and all  $q^* \in V$

$$\mathcal{L}(q_1, q_2, q^*) = (A_{22}q_2, q^*)_H + (A_{11}q_1, q^*)_H + (V_1, q^*)_H. \tag{16}$$

Its relation with the linear Hamiltonian function  $\mathcal{H}_{\text{LIN}}$  is

$$\mathcal{L}(q, \ddot{q}, \dot{q}) = \frac{d}{dt}[\mathcal{H}_{\text{LIN}}(q, \dot{q})]. \tag{17}$$

Equation (11) therefore transforms into seeking  $q : [0, T] \rightarrow V$  such that

$$\forall q^* \in V, \quad \mathcal{L}(q, \ddot{q}, \dot{q}, q^*) + \left[ \frac{d}{dt} \left( \frac{\partial \mathcal{L}_{\text{NL}}}{\partial q_2}(q, \dot{q}) \right) (q^*) - \frac{\partial \mathcal{L}_{\text{NL}}}{\partial q_1}(q, \dot{q})(q^*) \right] = Q(q, \dot{q}, q^*). \tag{18}$$

### 2.1. Quadratzation of Euler–Lagrange equations

Let us introduce a suitable auxiliary constant  $c \in \mathbb{R}_+^*$  and a scalar auxiliary variable  $z$ , depending only on time and not on space since  $\mathcal{H}_{\text{NL}}$  sends elements of  $V \times V$  to  $\mathbb{R}$ , and such that

$$z^2(t) = 2\mathcal{H}_{\text{NL}}(q, \dot{q}) + c. \tag{19}$$

Note that  $z$  is a real number. A derivation with respect to time gives

$$\dot{z}z = \frac{d}{dt}[\mathcal{H}_{\text{NL}}(q, \dot{q})] \tag{20}$$

$$= \frac{d}{dt}[\mathcal{I}_{\text{NL}}(q, \dot{q})] - \frac{d}{dt}[\mathcal{L}_{\text{NL}}(q, \dot{q})] \tag{21}$$

$$= \left[ \frac{d}{dt} \left( \frac{\partial \mathcal{L}_{\text{NL}}}{\partial q_2}(q, \dot{q}) \right) (\dot{q}) + \frac{\partial \mathcal{L}_{\text{NL}}}{\partial q_2}(q, \dot{q})(\ddot{q}) \right] - \left[ \frac{\partial \mathcal{L}_{\text{NL}}}{\partial q_2}(q, \dot{q})(\ddot{q}) + \frac{\partial \mathcal{L}_{\text{NL}}}{\partial q_1}(q, \dot{q})(\dot{q}) \right] \tag{22}$$

$$= \frac{d}{dt} \left( \frac{\partial \mathcal{L}_{\text{NL}}}{\partial q_2}(q, \dot{q}) \right) (\dot{q}) - \frac{\partial \mathcal{L}_{\text{NL}}}{\partial q_1}(q, \dot{q})(\dot{q}) \tag{23}$$

$$= \frac{\partial^2 \mathcal{L}_{\text{NL}}}{\partial q_2^2}(q, \dot{q})(\ddot{q})(\dot{q}) + \frac{\partial^2 \mathcal{L}_{\text{NL}}}{\partial q_1 \partial q_2}(q, \dot{q})(\dot{q})(\dot{q}) - \frac{\partial \mathcal{L}_{\text{NL}}}{\partial q_1}(q, \dot{q})(\dot{q}). \tag{24}$$

The so-called auxiliary function necessary for quadratzation is denoted  $G$  and writes

$$\begin{aligned} &\forall (q_1, q_2, q_3, q^*) \in V \times V \times H \times V, \quad G(q_1, q_2, q_3, q^*) \\ &= \frac{1}{\sqrt{2\mathcal{H}_{\text{NL}}(q_1, q_2) + c}} \left[ \frac{\partial^2 \mathcal{L}_{\text{NL}}}{\partial q_2^2}(q_1, q_2)(q_3) + \frac{\partial^2 \mathcal{L}_{\text{NL}}}{\partial q_1 \partial q_2}(q_1, q_2)(q_2) - \frac{\partial \mathcal{L}_{\text{NL}}}{\partial q_1}(q_1, q_2) \right] (q^*), \end{aligned} \tag{25}$$

which is a nonlinear form with respect to the first three arguments, and linear with respect to the last one  $q^*$ . The Euler–Lagrange equation (11) rewrites in a quadratized form: seek  $q : [0, T] \rightarrow V$  and  $z : [0, T] \rightarrow \mathbb{R}$  such that

$$\forall q^* \in V, \quad \begin{cases} \mathcal{L}(q, \ddot{q}, q^*) + zG(q, \dot{q}, \ddot{q}, q^*) = Q(q, \dot{q}, q^*), & (26a) \\ \dot{z} = G(q, \dot{q}, \ddot{q}, \dot{q}). & (26b) \end{cases}$$

**Theorem 2.4** (Power balance of the quadratized formulation (26)). *If the solution to (26) is regular enough, i.e.  $q \in C^1([0, T], V) \cap C^2([0, T], H)$  and  $z \in C^1([0, T], \mathbb{R})$ , it verifies*

$$\begin{cases} \frac{d\mathcal{E}}{dt} = Q(q, \dot{q}, \dot{q}), & (27a) \end{cases}$$

$$\begin{cases} \mathcal{E}(t) = \mathcal{H}_{\text{LIN}}(q, \dot{q}) + \frac{1}{2}z^2. & (27b) \end{cases}$$

*Proof.* If  $\dot{q} \in V$ , using  $q^* = \dot{q} \in V$  gives

$$\mathcal{L}(q, \ddot{q}, \dot{q}) + zG(q, \dot{q}, \ddot{q}, \dot{q}) = Q(q, \dot{q}, \dot{q}). \tag{28}$$

Then  $\mathcal{L}(q, \ddot{q}, \dot{q}) = \frac{d}{dt}[\mathcal{H}_{\text{LIN}}(q, \dot{q})]$  from equation (17), and  $G(q, \dot{q}, \ddot{q}, \dot{q}) = \dot{z}$  from equation (26b). □

Note that the second equation in (26) describes the evolution of the auxiliary variable and is a scalar equation. Unlike in the usual quadratization on potential energies, it is important to notice the presence of the time derivatives  $\dot{q}$  and  $\ddot{q}$  inside the nonlinear auxiliary function  $G$ . Even if the quadratization procedure described above is possible, the writing of an interesting linearly implicit numerical scheme with only explicit approximations as arguments of  $G$  is not straightforward.

### 2.2. Phase formulation of the equations

To achieve an efficient numerical integration strategy, let us rewrite the quadratized equations (26) in the phase space. To do so, two extra variables  $p_1 \in V$  and  $p_2 \in H$  are introduced such that  $p_1 = \dot{q}$  and  $p_2 = \dot{p}_1$  in the distribution sense. We now seek  $q : [0, T] \rightarrow V$ ,  $z : [0, T] \rightarrow \mathbb{R}$  and  $p_1, p_2$  two distributions such that

$$\forall q^* \in V, \quad \begin{cases} \dot{q} = p_1, & (29a) \\ \dot{p}_1 = p_2, & (29b) \\ \mathcal{L}(q, p_2, q^*) + zG(q, p_1, p_2, q^*) = Q(q, p_1, q^*), & (29c) \\ \dot{z} = G(q, p_1, p_2, p_1). & (29d) \end{cases}$$

Then a complete weak formulation of this system is proposed: seek  $(q, p_1, p_2, z) : [0, T] \rightarrow V \times V \times H \times \mathbb{R}$  such that

$$\begin{cases} \forall p_1^* \in V, \quad (\dot{q}, p_1^*)_V = (p_1, p_1^*)_V, & (30a) \\ \forall p_2^* \in H, \quad (\dot{p}_1, p_2^*)_H = (p_2, p_2^*)_H, & (30b) \\ \forall q^* \in V, \quad \mathcal{L}(q, p_2, q^*) + zG(q, p_1, p_2, q^*) = Q(q, p_1, q^*), & (30c) \\ \dot{z} = G(q, p_1, p_2, p_1). & (30d) \end{cases}$$

**Theorem 2.5** (Power balance of the phase quadratized formulation (30)). *If the solution of (30) is regular enough, i.e.  $q \in C^1([0, T], V)$ ,  $p_1 \in C^0([0, T], V) \cap C^1([0, T], H)$ ,  $p_2 \in C^0([0, T], H)$  and  $z \in C^1([0, T], \mathbb{R})$ , it verifies*

$$\begin{cases} \frac{d\mathcal{E}}{dt} = Q(q, p_1, p_1), & (31a) \end{cases}$$

$$\begin{cases} \mathcal{E} = \mathcal{H}_{\text{LIN}}(q, p_1) + \frac{1}{2}z^2. & (31b) \end{cases}$$

*Proof.* The weak formulation (30) is applied with  $q^* = p_1 \in V$ . This gives

$$\mathcal{L}(q, p_2, p_1) + zG(q, p_1, p_2, p_1) = Q(q, p_1, p_1). \tag{32}$$

Thanks to equation (30d) it writes

$$\mathcal{L}(q, p_2, p_1) + z\dot{z} = Q(q, p_1, p_1). \tag{33}$$

Now let's consider the linear term  $\mathcal{L}(q, p_2, p_1)$ . Thanks to equation (15) and symmetry of  $A_{22}$ , we have

$$\mathcal{L}(q, p_2, p_1) = (A_{22}p_2, p_1)_H + (A_{11}q, p_1)_H + (V_1, p_1)_H \tag{34}$$

$$= (A_{22}p_1, p_2)_H + (A_{11}q, p_1)_H + (V_1, p_1)_H. \tag{35}$$

Since  $p_1 \in V \subset H$ ,  $A_{22}p_1 \in H$ , equation (30b) with  $p_2^* = A_{22}p_1$  writes

$$(A_{22}p_1, p_2)_H = (A_{22}p_1, \dot{p}_1)_H. \tag{36}$$

Also, using  $p_1^* = q \in V$  in equation (30a) gives

$$(q, p_1)_V = (q, \dot{q})_V. \tag{37}$$

By definition of the inner product of  $V$  we have:

$$(A_{11}q, p_1)_H = (A_{11}q, \dot{q})_H. \tag{38}$$

Since  $A_{11}$  is bijective,  $V_1$  a unique antecedent  $X_1 \in V$  such that  $A_{11}X_1 = V_1$ . Using equation (30a) with  $p_2^* = X_1 \in V$  gives

$$(X_1, p_1)_V = (X_1, \dot{q})_V, \tag{39}$$

and so

$$(V_1, p_1)_H = (V_1, \dot{q})_H. \tag{40}$$

These combined results show that

$$\mathcal{L}(q, p_2, p_1) = (A_{22}p_1, \dot{p}_1)_H + (A_{11}q, \dot{q})_H + (V_1, \dot{q})_H \tag{41}$$

$$= \frac{d}{dt}[\mathcal{H}_{\text{LIN}}(q, p_1)]. \tag{42}$$

□

**Remark 2.6.** Note that equation (29c) is no longer an evolution equation. The evolution is contained in the extra equations (29a) and (29b).

**Remark 2.7.** The reformulation (29) allows to take advantage of the usual time discretization strategies used for potential energies quadratization. It is detailed in the next paragraph.

### 2.3. Discretization strategy

In order to write a time discretization of the quadratized equations, the time interval  $[0, T]$  is regularly divided with a step  $\Delta t$ . Let us introduce the discrete approximations

$$\mu q = \frac{q^{n+1} + q^n}{2}, \quad \delta q = \frac{q^{n+1} - q^n}{\Delta t}, \quad \pi q = \frac{1}{2}(3q^n - q^{n-1}). \tag{43}$$

and note that  $\pi$  is explicit, centered in  $(n + \frac{1}{2})\Delta t$  but depends only on past iterations, while  $\mu$  and  $\delta$  are centered in  $(n + \frac{1}{2})\Delta t$  in an implicit manner. We propose the following time integration scheme, which is linearly implicit. Find  $q^{n+1} \in V, p_1^{n+1} \in V, p_2^{n+1} \in H$  and  $z^{n+1} \in \mathbb{R}$  such that

$$\begin{cases} \forall p_1^* \in V, & (\delta q, p_1^*)_V = (\mu p_1, p_1^*)_V, & (44a) \\ \forall p_2^* \in H, & (\delta p_1, p_2^*)_H = (\mu p_2, p_2^*)_H, & (44b) \\ \forall q^* \in V, & \mathcal{L}(\mu q, \mu p_2, q^*) + \mu z G(\pi q, \pi p_1, \pi p_2, q^*) = Q(\mu q, \mu p_1, q^*), & (44c) \\ & \delta z = G(\pi q, \pi p_1, \pi p_2, \mu p_1). & (44d) \end{cases}$$

**Theorem 2.8** (Discrete power balance of the scheme (44)). *The solution to (44) verifies*

$$\begin{cases} \delta\mathcal{E} = Q(\mu q, \mu p_1, \mu p_1), \\ \mathcal{E}^n = \mathcal{H}_{\text{LIN}}(q^n, p_1^n) + \frac{1}{2}(z^n)^2. \end{cases} \tag{45a}$$

$$\tag{45b}$$

*Proof.* Let us use  $q^* = \mu p_1 \in V$  in equation (44c). Thanks to (44d) it is true that

$$\mu z G(\pi q, \pi p_1, \pi p_2, \mu p_1) = \mu z \delta z = \frac{1}{\Delta t} \left( \frac{1}{2}(z^{n+1})^2 - \frac{1}{2}(z^n)^2 \right). \tag{46}$$

This gives the expected result for the auxiliary variable  $z$ .

Now let us consider the term  $\mathcal{L}(\mu q, \mu p_2, \mu p_1)$ . Thanks to (15) and symmetry of  $A_{22}$ , it writes

$$\mathcal{L}(\mu q, \mu p_2, \mu p_1) = (A_{22}\mu p_2, \mu p_1)_H + (A_{11}\mu q, \mu p_1)_H + (V_1, \mu p_1)_H \tag{47}$$

$$= (A_{22}\mu p_1, \mu p_2)_H + (A_{11}\mu q, \mu p_1)_H + (V_1, \mu p_1)_H. \tag{48}$$

Since  $\mu p_1 \in V \subset H$ ,  $A_{22}\mu p_1 \in H$ , equation (44b) with  $p_2^* = A_{22}\mu p_1 \in H$  writes

$$(A_{22}\mu p_1, \mu p_2)_H = (A_{22}\mu p_1, \delta p_1)_H. \tag{49}$$

Also, using  $p_1^* = \mu q \in V$  in equation (44a) gives

$$(\mu q, \mu p_1)_V = (\mu q, \delta q)_V. \tag{50}$$

By definition of the inner product of  $V$  we have:

$$(A_{11}\mu q, \mu p_1)_H = (A_{11}\mu q, \delta q)_H. \tag{51}$$

Since  $A_{11}$  is bijective,  $V_1$  a unique antecedent  $X_1 \in V$  such that  $A_{11}X_1 = V_1$ . Using equation (44a) with  $p_2^* = X_1 \in V$  gives

$$(X_1, \mu p_1)_V = (X_1, \delta q)_V, \tag{52}$$

and so

$$(V_1, \mu p_1)_H = (V_1, \delta q)_H, \tag{53}$$

these results combined with the definition (12b) of the Hamiltonian show that:

$$\mathcal{L}(\mu q, \mu p_2, \mu p_1) = (A_{22}\mu p_1, \delta p_1)_H + (A_{11}\mu q, \delta q)_H + (V_1, \delta q)_H \tag{54}$$

$$= \frac{1}{\Delta t} [\mathcal{H}_{\text{LIN}}(q^{n+1}, p_1^{n+1}) - \mathcal{H}_{\text{LIN}}(q^n, p_1^n)]. \tag{55}$$

□

**Remark 2.9.** It is tempting to quadratize the whole equation (4) with no linear part  $\mathcal{L}$  left outside the quadratized function  $G$ . One would obtain

$$\forall q^* \in V, \begin{cases} zG(q, \dot{q}, \ddot{q}, q^*) = Q(q, \dot{q}, q^*), \\ \dot{z} = G(q, \dot{q}, \ddot{q}, \dot{q}), \end{cases} \tag{56a}$$

$$\tag{56b}$$

and the associated scheme would be

$$\begin{cases} \forall p_1^* \in V, & (\delta q, p_1^*)_V = (\mu p_1, p_1^*)_V, \end{cases} \tag{57a}$$

$$\begin{cases} \forall p_2^* \in H, & (\delta p_1, p_2^*)_H = (\mu p_2, p_2^*)_H, \end{cases} \tag{57b}$$

$$\begin{cases} \forall q^* \in V, & \mu z G(\pi q, \pi p_1, \pi p_2, q^*) = Q(\mu q, \mu p_1, q^*), \end{cases} \tag{57c}$$

$$\begin{cases} \delta z = G(\pi q, \pi p_1, \pi p_2, \mu p_1). \end{cases} \tag{57d}$$

In the absence of dissipation and constraints, *i.e.* if  $Q(\mu q, \mu p_1, \cdot)$  is independent of the unknowns, this scheme is not invertible and therefore unusable in practice. To avoid this pitfall, there should always be a part of the linear terms outside the quadratization. In theory, leaving any proportion of the linear part is enough to make the system invertible. However, numerical experiments should be carried out to verify the behavior of the scheme

in these situations where the linear part tends to be completely absorbed by the quadratization, and maybe to find an optimal balance.

### 3. APPLICATION TO A ROTATING FLEXIBLE PIANO HAMMER

In a piano, the mechanical action of the player is converted into vibro-acoustic waves by an ingenious mechanism that allows the strings to be struck by hammers without being muffled by them.

The pianist operates the key, which in turn sets in motion several elements that generate a force on the hammer shank, as illustrated in Figure 1. This force rotates the hammer and enables the head to strike the strings. It also causes a bending of the shank that could depend on the acceleration profile imposed by the pianist on the key, and thus explain the influence of the pianistic touch on the sound [9, 18, 33]. For this reason, accurate modeling and efficient resolution of the vibrating shank is essential.

#### 3.1. Physical model

In the following we use the physical model derived in [9]. The piano hammer is modeled as a Timoshenko 1D beam of length  $L$  and section  $S$  submitted to gravity  $-g\mathbf{u}_y$  and to which two exterior forces apply

- $\mathbf{F}_{\text{meca}}$  the force coming from the input of the pianist and transmitted through the action;
- $\mathbf{F}_{\text{coupl}}$  the force of the hammer head on the hammer shank.

The hammer head is considered as a second separate body acting on the shank through the force  $\mathbf{F}_{\text{coupl}}$  and on which the obstacle (usually strings) exerts a force  $\mathbf{F}_{\text{obs}}$ . Other parameters are the density  $\rho$ , the Young modulus  $E$ , the shear modulus  $G$ , the quadratic momentum  $I$ , and  $\kappa$  is a Timoshenko coefficient. Small deformations are supposed so that the theory of Timoshenko holds.

Because of the flexibility of the shank, the definition of the rotation angle  $\theta$  of the rotating frame  $(\mathbf{u}_r, \mathbf{u}_\theta)$  with respect to the fixed frame  $(\mathbf{u}_x, \mathbf{u}_y)$  is not unique. The choice is made to define this angle with respect to a zero-average bending position

$$\int_0^L w(x) dx = 0, \tag{58}$$

and this constraint is enforced with a Lagrange multiplier  $\lambda$ . In the Cartesian frame  $(\mathbf{u}_x, \mathbf{u}_y)$ , the rotating vectors  $\mathbf{u}_r$  and  $\mathbf{u}_\theta$  write

$$\mathbf{u}_r = \begin{pmatrix} \cos \theta \\ \sin \theta \end{pmatrix}, \quad \mathbf{u}_\theta = \begin{pmatrix} \sin \theta \\ -\cos \theta \end{pmatrix}. \tag{59}$$

The motion of the center of gravity of the head with mass  $m_H$ , located at a height  $H$  above the shank, is described by the position vector  $\boldsymbol{\xi}$ , see Figure 2. The contact with the obstacle happens when  $d = \boldsymbol{\xi} \cdot \mathbf{u}_y \leq d_0$ .

Let  $\mathcal{H} = L^2([0, L])$  and  $\mathcal{V}_0$  be the functions of  $\mathcal{V} = H^1([0, L])$  such that

$$\mathcal{V}_0 = \{ w \in H^1([0, L]) \mid w(0) = 0 \}. \tag{60}$$

The following model derived in [9] is obtained with the virtual work principle applied to the shank.

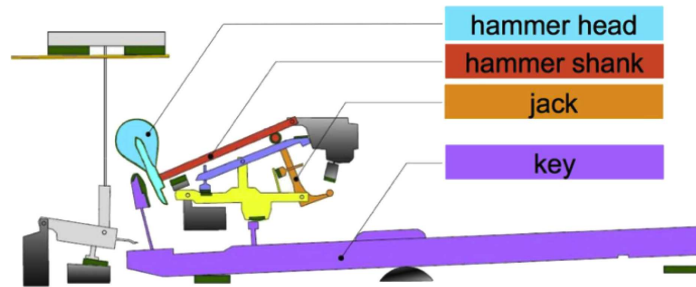


FIGURE 1. Sketch of the different parts of a grand piano action, from [9].

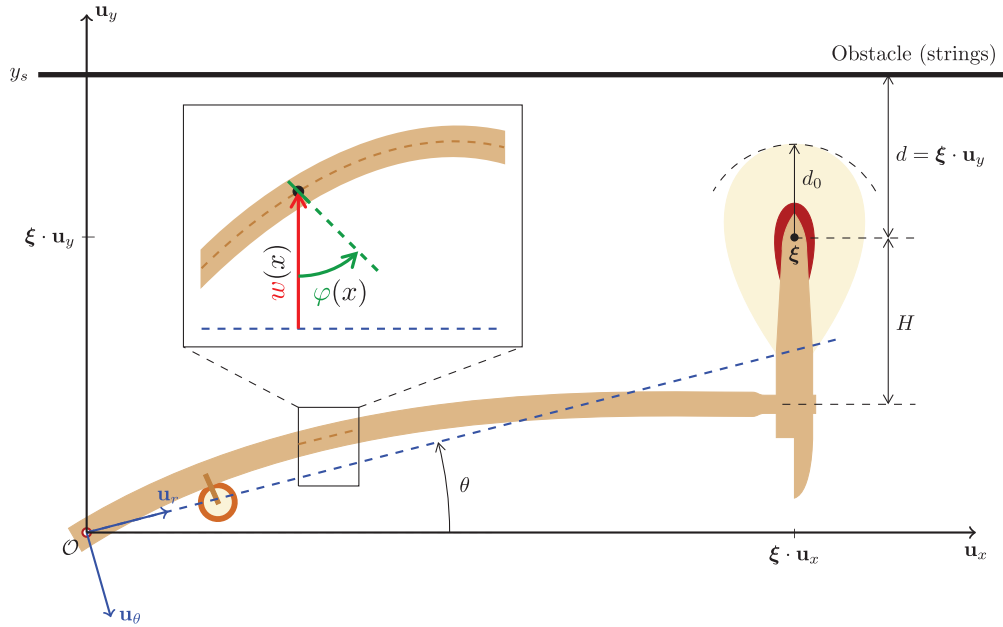


FIGURE 2. Flexible hammer parametrization.

It consists in seeking  $(w, \varphi, \theta, \lambda, \mathbf{F}_{\text{coupl}}, \xi) : [0, T] \rightarrow \mathcal{V}_0 \times \mathcal{V} \times \mathbb{R} \times \mathbb{R} \times \mathbb{R}^2 \times \mathbb{R}^2$ , so that for all  $(w^*, \varphi^*) \in \mathcal{V}_0 \times \mathcal{V}$

$$\left\{ \begin{array}{l} \text{Shank equations:} \\ \int_0^L \rho S \ddot{w} w^* + \int_0^L SG \kappa (\partial_x w - \varphi) \partial_x w^* + \lambda \int_0^L w^* \\ \quad - \int_0^L \rho S (w \dot{\theta}^2 + \ddot{\theta} x + g \cos \theta) w^* = (\mathbf{F}_{\text{coupl}} \cdot \mathbf{u}_\theta) w^*(L) + f_w(w^*), \end{array} \right. \quad (61a)$$

$$\left\{ \begin{array}{l} \int_0^L \rho I \ddot{\varphi} \varphi^* + \int_0^L SG \kappa (\partial_x w - \varphi) \varphi^* + \int_0^L EI \partial_x \varphi \partial_x \varphi^* - \rho I \ddot{\theta} \int_0^L \varphi^* = f_\varphi(\varphi^*), \end{array} \right. \quad (61b)$$

$$\left\{ \begin{array}{l} \text{Zero mean-value of the flexion / Equation on } \lambda: \\ \int_0^L w = 0, \end{array} \right. \quad (61c)$$

$$\left\{ \begin{array}{l} \text{Equation on } \theta: \\ \ddot{\theta} \int_0^L \rho S (w^2 + x^2) + 2\dot{\theta} \int_0^L \rho S w \dot{w} + \int_0^L \rho I (\ddot{\theta} - \ddot{\varphi}) - \int_0^L \rho S x \ddot{w} \\ \quad + \int_0^L \rho S g (x \cos \theta + w \sin \theta) = (w(L) - H)(\mathbf{F}_{\text{coupl}} \cdot \mathbf{u}_r) - L(\mathbf{F}_{\text{coupl}} \cdot \mathbf{u}_\theta) + f_\theta, \end{array} \right. \quad (61d)$$

$$\left\{ \begin{array}{l} \text{Equation of the hammer head (Newton's law):} \\ m_H \ddot{\xi} = -m_H g \mathbf{u}_y - \mathbf{F}_{\text{coupl}} - \mathbf{F}_{\text{obs}}, \end{array} \right. \quad (61e)$$

$$\left\{ \begin{array}{l} \text{Shank-Head continuity:} \\ \xi = L \mathbf{u}_r + (w(L) - H) \mathbf{u}_\theta. \end{array} \right. \quad (61f)$$

The initial conditions at  $t = 0$  are given by

$$\begin{cases} \forall x \in [0, L], & w(x, 0) = 0, \\ \forall x \in [0, L], & \varphi(x, 0) = 0, \\ \theta(0) = \theta_0, \\ \boldsymbol{\xi}(0) = L \begin{pmatrix} \cos \theta_0 \\ \sin \theta_0 \end{pmatrix} - H \begin{pmatrix} \sin \theta_0 \\ -\cos \theta_0 \end{pmatrix}. \end{cases} \tag{62}$$

The force  $\mathbf{F}_{\text{meca}}$ , coming from the action, is here represented by the source terms  $f_w, f_\varphi$  and  $f_\theta$ .

**Remark 3.1.** For a usual linear Timoshenko system, the Hille–Yosida theorem ensures the existence and uniqueness of a strong solution in  $(w, \varphi) \in C^1([0, T], \mathcal{V}_0 \times \mathcal{V}) \cap C^2([0, T], \mathcal{H}^2)$  (see [7]). To the best of our knowledge, there is no proof of such a result for the model (61), but the considered nonlinearity remains weak enough so that we will look for solutions in the same spaces nonetheless for this paper. The maximal-dissipative character of the evolution operator, necessary to apply Hille–Yosida theorem, is closely related to the following power balance, but would necessitate a further analysis. Note that well-posedness is obtained for Euler–Bernoulli blades with an imposed rotation in [24].

**Theorem 3.2** (Power balance of the rotating shank (61)). *If the solution to (61) is regular enough, i.e.  $(w, \varphi) \in C^1([0, T], \mathcal{V}_0 \times \mathcal{V}) \cap C^2([0, T], \mathcal{H}^2)$ , it verifies*

$$\begin{cases} \frac{d\mathcal{E}}{dt} = f_w(\dot{w}) + f_\varphi(\dot{\varphi}) + f_\theta \dot{\theta} - \mathbf{F}_{\text{string}} \cdot \dot{\boldsymbol{\xi}}, & \tag{63a} \\ \mathcal{E} = \frac{1}{2} \int_0^L \rho S w^2 \dot{\theta}^2 dx + \frac{1}{2} \int_0^L \rho S (\dot{w} - x \dot{\theta})^2 dx + \frac{1}{2} \int_0^L \rho I (\dot{\theta} - \dot{\varphi})^2 dx \\ \quad + \frac{1}{2} \int_0^L S G \kappa (\partial_x w - \varphi)^2 dx + \frac{1}{2} \int_0^L E I \partial_x \varphi^2 dx & \tag{63b} \\ \quad + \int_0^L \rho S g (x \sin \theta - w \cos \theta) dx + \frac{1}{2} m_H |\dot{\boldsymbol{\xi}}|^2 + m_H g \boldsymbol{\xi} \cdot \mathbf{u}_y. \end{cases}$$

*Proof.* Use the weak formulation (61) with  $w^* = \dot{w} \in \mathcal{V}_0, \varphi^* = \dot{\varphi} \in \mathcal{V}$  and multiply the equation on  $\theta$  by  $\dot{\theta}$ .  $\square$

**Remark 3.3.** Dissipative terms can be added to the equations (61). For example, damping terms internal to the shank, or a dissipation term associated with the  $\theta$  angle and due to friction in the pivot link. For the sake of readability, we neglect them here, as they can be treated independently from the quadratization process.

**Remark 3.4.** Notice that system (61) leads to a power balance (63) where the nonlinear terms of the kinetic energy are not distributed over space, but are rather related to the scalar unknown  $\theta$ . Hence this application case only illustrates part of the possibilities covered by scheme (44). More intricate models with a distributed nonlinear kinetic energy could be the object of future work.

### 3.2. Scalar Lagrangian Quadratization

The energy of Theorem 3.2 is mostly a quadratic form, but also has two nonlinear energy terms. The term  $\int_0^L \rho S g (x \sin(\theta) - w \cos(\theta)) dx$  is a potential nonlinear energy, and  $\frac{1}{2} \int_0^L \rho S w^2 \dot{\theta}^2 dx$  brings a nonlinear kinetic contribution. In order to quadratize the system, the Lagrangian method resented in Section 2 is applied. The

nonlinear Lagrangian and Hamiltonian read, for any  $(w_1, w_2, \varphi_1, \varphi_2, \theta_1, \theta_2, \theta_3) \in \mathcal{V}_0^2 \times \mathcal{V}^2 \times \mathbb{R}^3$ ,

$$\begin{cases} \mathcal{L}(w_1, \varphi_1, w_2, \varphi_2, \theta_1, \theta_2) = \frac{1}{2} \int_0^L \rho S w_1^2 \theta_2^2 \, dx - \int_0^L \rho S g(x \sin \theta_1 - w_1 \cos \theta_1) \, dx, & (64a) \\ \mathcal{H}(w_1, \varphi_1, w_2, \varphi_2, \theta_1, \theta_2) = \frac{1}{2} \int_0^L \rho S w_1^2 \theta_2^2 \, dx + \int_0^L \rho S g(x \sin \theta_1 - w_1 \cos \theta_1) \, dx. & (64b) \end{cases}$$

**Remark 3.5.** These Lagrangian and Hamiltonian are linked by the relation (1). It should also be remarked that they do not depend on the second argument of the distributed variables  $w_2$  and  $\varphi_2$ , but only on the variable  $\theta_2$  which is scalar.

**Remark 3.6.** Because of the constraint (58), the solution to (61) satisfies

$$\int_0^L \rho S g(x \sin \theta - w \cos \theta) \, dx = \frac{1}{2} \rho S g L^2 \sin \theta, \tag{65}$$

which is lower bounded.

Following (19), let us introduce a constant  $c \in \mathbb{R}_+^*$  and define the auxiliary variable as

$$\forall t \in [0, T], \quad z(t) \equiv \sqrt{2\mathcal{H}(w, \varphi, \dot{w}, \dot{\varphi}, \theta, \dot{\theta})} + c. \tag{66}$$

The nonlinear Euler–Lagrange term of the equations is defined for any  $(w_1, w_2, w^*, \varphi_1, \varphi_2, \varphi^*, \theta_1, \theta_2, \theta_3, \theta^*) \in \mathcal{V}_0^3 \times \mathcal{V}^3 \times \mathbb{R}^4$ , as

$$\begin{aligned} & EL(w_1, \varphi_1, w_2, \varphi_2, \theta_1, \theta_2, \theta_3, w^*, \varphi^*, \theta^*) \\ &= \int_0^L \left[ \rho S \begin{pmatrix} -w_1 \theta_2^2 \\ 0 \\ 2w_1 w_2 \theta_2 + w_1^2 \theta_3 \end{pmatrix} + \rho S g \begin{pmatrix} -\cos \theta_1 \\ 0 \\ x \cos \theta_1 + w_1 \sin \theta_1 \end{pmatrix} \right] \cdot \begin{pmatrix} w^* \\ \varphi^* \\ \theta^* \end{pmatrix} \, dx, \end{aligned} \tag{67}$$

and following (25), the quadratization auxiliary function is defined as

$$G(w_1, \varphi_1, w_2, \varphi_2, \theta_1, \theta_2, \theta_3, w^*, \varphi^*, \theta^*) = \frac{EL(w_1, \varphi_1, w_2, \varphi_2, \theta_1, \theta_2, \theta_3, w^*, \varphi^*, \theta^*)}{\sqrt{2\mathcal{H}(w_1, \varphi_1, w_2, \varphi_2, \theta_1, \theta_2)} + c}. \tag{68}$$

Let us introduce the matrices and vectors

$$M = \begin{pmatrix} \rho S & 0 \\ 0 & \rho I \end{pmatrix}, \quad A = \begin{pmatrix} SG\kappa & 0 \\ 0 & EI \end{pmatrix}, \quad B = \begin{pmatrix} 0 & -SG\kappa \\ 0 & 0 \end{pmatrix}, \quad C = \begin{pmatrix} 0 & 0 \\ 0 & SG\kappa \end{pmatrix}, \quad f_q = \begin{pmatrix} f_w \\ f_\varphi \end{pmatrix}, \tag{69}$$

and a vectorial unknown  $q = {}^t(w, \varphi)$ . The model (61) rewrites: seek  $(q, \theta, \lambda, \mathbf{F}_{\text{coupl}}, \boldsymbol{\xi}) : [0, T] \rightarrow \mathcal{V}_0 \times \mathcal{V} \times \mathbb{R} \times \mathbb{R} \times \mathbb{R}^2 \times \mathbb{R}^2$  so that for all  $q^* \in \mathcal{V}_0 \times \mathcal{V}$

$$\left\{ \begin{array}{l}
 \int_0^L M\ddot{q} \cdot q^* + \int_0^L Cq \cdot q^* + \int_0^L Bq \cdot \partial_x q^* + \int_0^L {}^t B \partial_x q \cdot q^* + \int_0^L A \partial_x q \cdot \partial_x q^* - \ddot{\theta} \int_0^L M \begin{pmatrix} x \\ 1 \end{pmatrix} \cdot q^* \\
 \quad + \lambda \int_0^L q^* \cdot \begin{pmatrix} 1 \\ 0 \end{pmatrix} + EL(q, \dot{q}, \theta, \dot{\theta}, \ddot{\theta}, q^*, 0) = (\mathbf{F}_{\text{coupl}} \cdot \mathbf{u}_\theta) q^*(L) \cdot \begin{pmatrix} 1 \\ 0 \end{pmatrix} + f_q(q^*), \tag{70a} \\
 \\
 \int_0^L q \cdot \begin{pmatrix} 1 \\ 0 \end{pmatrix} = 0, \tag{70b} \\
 \\
 \ddot{\theta} \int_0^L M \begin{pmatrix} x \\ 1 \end{pmatrix} \cdot \begin{pmatrix} x \\ 1 \end{pmatrix} - \int_0^L M \begin{pmatrix} x \\ 1 \end{pmatrix} \cdot \ddot{q} + EL(q, \dot{q}, \theta, \dot{\theta}, \ddot{\theta}, 0, 1) \\
 \quad = \left( q(L) \cdot \begin{pmatrix} 1 \\ 0 \end{pmatrix} - H \right) (\mathbf{F}_{\text{coupl}} \cdot \mathbf{u}_r) - L(\mathbf{F}_{\text{coupl}} \cdot \mathbf{u}_\theta) + f_\theta, \tag{70c} \\
 \\
 m_H \ddot{\boldsymbol{\xi}} = -m_H g \mathbf{u}_y - \mathbf{F}_{\text{coupl}} - \mathbf{F}_{\text{obs}}, \tag{70d} \\
 \\
 \boldsymbol{\xi} = L \mathbf{u}_r + \left( q(L) \cdot \begin{pmatrix} 1 \\ 0 \end{pmatrix} - H \right) \mathbf{u}_\theta. \tag{70e}
 \end{array} \right.$$

Thanks to the auxiliary function (68) and the auxiliary variable (66), a quadratized formulation writes: seek  $(q, \theta, \lambda, z, \mathbf{F}_{\text{coupl}}, \boldsymbol{\xi}) : [0, T] \rightarrow \mathcal{V}_0 \times \mathcal{V} \times \mathbb{R} \times \mathbb{R} \times \mathbb{R} \times \mathbb{R}^2 \times \mathbb{R}^2$  so that for all  $q^* \in \mathcal{V}_0 \times \mathcal{V}$

$$\left\{ \begin{array}{l}
 \int_0^L M\ddot{q} \cdot q^* + \int_0^L Cq \cdot q^* + \int_0^L Bq \cdot \partial_x q^* + \int_0^L {}^t B \partial_x q \cdot q^* + \int_0^L A \partial_x q \cdot \partial_x q^* - \ddot{\theta} \int_0^L M \begin{pmatrix} x \\ 1 \end{pmatrix} \cdot q^* \\
 \quad + \lambda \int_0^L q^* \cdot \begin{pmatrix} 1 \\ 0 \end{pmatrix} + zG(q, \dot{q}, \theta, \dot{\theta}, \ddot{\theta}, q^*, 0) = (\mathbf{F}_{\text{coupl}} \cdot \mathbf{u}_\theta) q^*(L) \cdot \begin{pmatrix} 1 \\ 0 \end{pmatrix} + f_q(q^*), \tag{71a} \\
 \\
 \int_0^L q \cdot \begin{pmatrix} 1 \\ 0 \end{pmatrix} = 0, \tag{71b} \\
 \\
 \ddot{\theta} \int_0^L M \begin{pmatrix} x \\ 1 \end{pmatrix} \cdot \begin{pmatrix} x \\ 1 \end{pmatrix} - \int_0^L M \begin{pmatrix} x \\ 1 \end{pmatrix} \cdot \ddot{q} + zG(q, \dot{q}, \theta, \dot{\theta}, \ddot{\theta}, 0, 1) \\
 \quad = \left( q(L) \cdot \begin{pmatrix} 1 \\ 0 \end{pmatrix} - H \right) (\mathbf{F}_{\text{coupl}} \cdot \mathbf{u}_r) - L(\mathbf{F}_{\text{coupl}} \cdot \mathbf{u}_\theta) + f_\theta, \tag{71c} \\
 \\
 \dot{z} = G(q, \dot{q}, \theta, \dot{\theta}, \ddot{\theta}, \dot{q}, \dot{\theta}), \tag{71d} \\
 \\
 m_H \ddot{\boldsymbol{\xi}} = -m_H g \mathbf{u}_y - \mathbf{F}_{\text{coupl}} - \mathbf{F}_{\text{obs}}, \tag{71e} \\
 \\
 \boldsymbol{\xi} = L \mathbf{u}_r + \left( q(L) \cdot \begin{pmatrix} 1 \\ 0 \end{pmatrix} - H \right) \mathbf{u}_\theta. \tag{71f}
 \end{array} \right.$$

Following the process of Section 2, the phase formulation of these hamper equations writes:

find  $(q, p, \theta, T_1, T_2, \lambda, z, \mathbf{F}_{\text{coupl}}, \boldsymbol{\xi}, \mathbf{X}) : [0, T] \rightarrow (\mathcal{V}_0 \times \mathcal{V})^2 \times \mathbb{R}^5 \times (\mathbb{R}^2)^3$  so that for all  $q^* \in \mathcal{V}_0 \times \mathcal{V}$  and  $p^* \in \mathcal{V}_0 \times \mathcal{V}$ ,

$$\left\{ \begin{array}{l} \dot{\theta} = T_1, \end{array} \right. \tag{72a}$$

$$\left\{ \begin{array}{l} \dot{T}_1 = T_2, \end{array} \right. \tag{72b}$$

$$\left\{ \begin{array}{l} \int_0^L C\dot{q} \cdot p^* + \int_0^L B\dot{q} \cdot \partial_x p^* + \int_0^L {}^t B \partial_x \dot{q} \cdot p^* + \int_0^L A \partial_x \dot{q} \cdot \partial_x p^* \\ = \int_0^L Cp \cdot p^* + \int_0^L Bp \cdot \partial_x p^* + \int_0^L {}^t B \partial_x p \cdot p^* + \int_0^L A \partial_x p \cdot \partial_x p^*, \end{array} \right. \tag{72c}$$

$$\left\{ \begin{array}{l} \int_0^L M\dot{p} \cdot q^* + \int_0^L Cq \cdot q^* + \int_0^L Bq \cdot \partial_x q^* + \int_0^L {}^t B \partial_x q \cdot q^* + \int_0^L A \partial_x q \cdot \partial_x q^* - T_2 \int_0^L M \begin{pmatrix} x \\ 1 \end{pmatrix} \cdot q^* \\ + \lambda \int_0^L q^* \cdot \begin{pmatrix} 1 \\ 0 \end{pmatrix} + zG(q, p, \theta, T_1, T_2, q^*, 0) = (\mathbf{F}_{\text{coupl}} \cdot \mathbf{u}_\theta)q^*(L) \cdot \begin{pmatrix} 1 \\ 0 \end{pmatrix} + f_q(q^*), \end{array} \right. \tag{72d}$$

$$\left\{ \begin{array}{l} \int_0^L q \cdot \begin{pmatrix} 1 \\ 0 \end{pmatrix} = 0, \end{array} \right. \tag{72e}$$

$$\left\{ \begin{array}{l} T_2 \int_0^L M \begin{pmatrix} x \\ 1 \end{pmatrix} \cdot \begin{pmatrix} x \\ 1 \end{pmatrix} - \int_0^L M \begin{pmatrix} x \\ 1 \end{pmatrix} \cdot \dot{p} + zG(q, p, \theta, T_1, T_2, 0, 1) \\ = \left( q(L) \cdot \begin{pmatrix} 1 \\ 0 \end{pmatrix} - H \right) (\mathbf{F}_{\text{coupl}} \cdot \mathbf{u}_r) - L(\mathbf{F}_{\text{coupl}} \cdot \mathbf{u}_\theta) + f_\theta, \end{array} \right. \tag{72f}$$

$$\left\{ \begin{array}{l} \dot{z} = G(q, \dot{q}, \theta, \dot{\theta}, \ddot{\theta}, \dot{q}, \dot{\theta}), \end{array} \right. \tag{72g}$$

$$\left\{ \begin{array}{l} \dot{\boldsymbol{\xi}} = \mathbf{X}, \end{array} \right. \tag{72h}$$

$$\left\{ \begin{array}{l} m_H \dot{\mathbf{X}} = -m_H g \mathbf{u}_y - \mathbf{F}_{\text{coupl}} - \mathbf{F}_{\text{obs}}, \end{array} \right. \tag{72i}$$

$$\left\{ \begin{array}{l} \mathbf{X} = T_1 \left( q(L) \cdot \begin{pmatrix} 1 \\ 0 \end{pmatrix} - H \right) \mathbf{u}_r + \left( p(L) \cdot \begin{pmatrix} 1 \\ 0 \end{pmatrix} - LT_1 \right) \mathbf{u}_\theta. \end{array} \right. \tag{72j}$$

The equation  $\dot{q} = p$  is written in the weak form (72c) with the scalar product associated to the bilinear form

$$\forall (u, v) \in (\mathcal{V} \times \mathcal{V}_0)^2, \quad a(u, v) = \int_0^L Cu \cdot v + \int_0^L Bu \cdot \partial_x v + \int_0^L {}^t B \partial_x u \cdot v + \int_0^L A \partial_x u \cdot \partial_x v. \tag{73}$$

which can be represented by Riesz theorem by an operator  $A_{11}$  similar to the one defined in Section 2.

**Remark 3.7.** Note that the present system does not need a variational equation like (30b) because the nonlinear term actually does not depend on the second derivatives in time of the distributed unknowns. Only an equivalent scalar form for the scalar variable  $\theta$  is necessary, leading to (72b).



The space discretized model writes in the phase formulation:

find  $(Q_h, P_h, \theta_h, T_{h,1}, T_{h,2}, \lambda_h, z_h, \mathbf{F}_{\text{coupl}}, \boldsymbol{\xi}_h, \mathbf{X}_h) \in \mathbb{R}^{2n_h} \times \mathbb{R}^{2n_h} \times \mathbb{R}^5 \times (\mathbb{R}^2)^3$  such that

$$\left\{ \begin{array}{l} \dot{\theta}_h = T_{1,h}, \tag{76a} \\ \dot{T}_{1,h} = T_{h,2}, \tag{76b} \\ {}^t K_h \dot{Q}_h = {}^t K_h P_h \quad \left( \iff \dot{Q}_h = P_h \text{ since } K_h \text{ is invertible} \right), \tag{76c} \\ M_h \dot{P}_h + K_h Q_h - T_{h,2} M_h V_h + \lambda_h I_h^w + z_h \mathbb{G}_q(Q_h, P_h, \theta_h, T_{1,h}, T_{h,2}) \\ \qquad \qquad \qquad = (\mathbf{F}_{\text{coupl}} \cdot \mathbf{u}_\theta) I_h^{w(L)} + F_{h,Q}, \tag{76d} \\ I_h^w \cdot Q_h = 0, \tag{76e} \\ T_{h,2} M_h V_h \cdot V_h - M_h V_h \cdot \dot{P}_h + z_h \mathbb{G}_\theta(Q_h, P_h, \theta_h, T_{h,1}, T_{h,2}) \\ \qquad \qquad \qquad = (Q_h \cdot I_h^{w(L)} - H) (\mathbf{F}_{\text{coupl}} \cdot \mathbf{u}_r) - L(\mathbf{F}_{\text{coupl}} \cdot \mathbf{u}_\theta) + F_{h,\theta}, \tag{76f} \\ \dot{z}_h = \mathbb{G}_q(Q_h, P_h, \theta_h, T_{h,1}, T_{h,2}) \cdot P_h + \mathbb{G}_\theta(Q_h, P_h, \theta_h, T_{h,1}, T_{h,2}) T_{h,1}, \tag{76g} \\ \dot{\boldsymbol{\xi}}_h = \mathbf{X}_h, \tag{76h} \\ m_H \dot{\mathbf{X}}_h = -m_H g \mathbf{u}_y - \mathbf{F}_{\text{coupl}} - \mathbf{F}_{\text{obs}}, \tag{76i} \\ \mathbf{X}_h = T_{h,1} (Q_h \cdot I_h^{w(L)} - H) \mathbf{u}_r + (P_h \cdot I_h^{w(L)} - L T_{h,1}) \mathbf{u}_\theta. \tag{76j} \end{array} \right.$$

### 3.4. Time discretization

#### 3.4.1. Force coming from the obstacle

The coupling with real nonlinear piano strings is beyond the scope of this article (see [5] for details about numerical methods for the strings). The focus is on the shank itself and so it will be considered that the hammer impacts a rigid obstacle located at the height  $y_s$ .

The force  $\mathbf{F}_{\text{obs}}$  models the crushing of the hammer made of felt, as (see [7, 9, 31])

$$F_{\text{obs}} = \mathbf{F}_{\text{obs}} \cdot \mathbf{u}_y = \Phi(\boldsymbol{\xi} \cdot \mathbf{u}_y), \quad \Phi(\xi_y) = K \left[ (d_0 + \xi_y - y_s)^+ \right]^p, \tag{77}$$

where  $p$  is a positive real number that quantifies the nonlinear effects,  $K$  is a stiffness parameter of the hammer felt, and  $(\cdot)^+$  stands for the positive part.

**Remark 3.8.** For the same reasons as before (see Rem. 3.3) the dissipative terms of the interaction is neglected in this paper. Moreover, the hammer does not have any interaction with the obstacle in the horizontal direction. Such friction motion (see [33]) is a way to transmit the vibrations of the shank and could allow the pianist to influence the longitudinal modes of the string with his touch. This is left for future studies.

Since the function  $\Phi$  is nonlinear, a classical potential quadratization is applied following [15]. Let  $\Psi$  be the primitive function of  $\Phi$  such that:

$$\forall y \in \mathbb{R}, \quad \Psi(y) = \int_{-\infty}^y \Phi(s) ds. \tag{78}$$

Let us introduce a constant  $c_H > 0$ . The auxiliary variable for the hammer head is  $z_H = \sqrt{2\Phi(\xi_y) + c_H}$  and  $G_H$  is the quadratization auxiliary function defined as

$$\forall y \in \mathbb{R}, \quad G_H(y) = \frac{\Phi(y)}{\sqrt{2\Psi(y) + c_H}}, \tag{79}$$

so that

$$\mathbf{F}_{\text{obs}} \cdot \mathbf{u}_y = z_H G_H(\boldsymbol{\xi} \cdot \mathbf{u}_y) \quad \text{and} \quad \dot{z}_H = G_H(\boldsymbol{\xi} \cdot \mathbf{u}_y) \dot{\boldsymbol{\xi}} \cdot \mathbf{u}_y = G_H(\boldsymbol{\xi} \cdot \mathbf{u}_y) \mathbf{X} \cdot \mathbf{u}_y, \tag{80}$$

with  $\mathbf{X} = \dot{\boldsymbol{\xi}}$ .

3.4.2. Scalar Lagrangian Quadraticization (SLQ) scheme

Using the notations (43) for discrete time approximations, the following linearly implicit time scheme is derived: find  $(Q_h^{n+1}, P_h^{n+1}, \theta_h^{n+1}, T_{h,1}^{n+1}, T_{h,2}^{n+1}, \lambda_h, z_h^{n+1}, \mathbf{F}_{\text{coupl}}, \boldsymbol{\xi}_h^{n+1}, \mathbf{X}_h^{n+1}, z_{Hh}^{n+1}) \in \mathbb{R}^{2n_h} \times \mathbb{R}^{2n_h} \times \mathbb{R}^5 \times (\mathbb{R}^2)^3 \times \mathbb{R}$  so that

$$\left\{ \begin{array}{l} \delta\theta_h = \mu T_{h,1}, \tag{81a} \\ \delta T_{h,1} = \mu T_{h,2}, \tag{81b} \\ \delta Q_h = \mu P_h, \tag{81c} \\ M_h \delta P_h + K_h \mu Q_h - \mu T_{h,2} M_h V_h + \lambda_h I_h^w + \mu z_h \mathbb{G}_q(\pi Q_h, \pi P_h, \pi \theta_h, \pi T_{h,1}, \pi T_{h,2}) \\ \qquad \qquad \qquad = (\mathbf{F}_{\text{coupl}} \cdot \pi \mathbf{u}_\theta) I_h^{w(L)} + F_{h,Q}^{n+1/2}, \tag{81d} \\ I_h^w \cdot \mu Q_h = 0, \tag{81e} \\ \mu T_{h,2} M_h V_h \cdot V_h - M_h V_h \cdot \delta P_h + \mu z_h \mathbb{G}_\theta(\pi Q_h, \pi P_h, \pi \theta_h, \pi T_{h,1}, \pi T_{h,2}) \\ \qquad \qquad \qquad = (\pi Q_h \cdot I_h^{w(L)} - H) (\mathbf{F}_{\text{coupl}} \cdot \pi \mathbf{u}_r) - L (\mathbf{F}_{\text{coupl}} \cdot \pi \mathbf{u}_\theta) + F_{h,\theta}^{n+1/2}, \tag{81f} \\ \delta z_h = \mathbb{G}_q(\pi Q_h, \pi P_h, \pi \theta_h, \pi T_{h,1}, \pi T_{h,2}) \cdot \mu P_h + \mathbb{G}_\theta(\pi Q_h, \pi P_h, \pi \theta_h, \pi T_{h,1}, \pi T_{h,2}) \mu T_{h,1}, \tag{81g} \\ \delta \boldsymbol{\xi}_h = \mu \mathbf{X}_h, \tag{81h} \\ m_H \delta \mathbf{X}_h = -m_H g \mathbf{u}_y - \mathbf{F}_{\text{coupl}} - F_{\text{obs}} \mathbf{u}_y, \tag{81i} \\ \mu \mathbf{X}_h = \mu T_{h,1} (\pi Q_h \cdot I_h^{w(L)} - H) \pi \mathbf{u}_r + (\mu P_h \cdot I_h^{w(L)} - L \mu T_{h,1}) \pi \mathbf{u}_\theta, \tag{81j} \\ F_{\text{obs}} = \mu z_H G_H(\pi \boldsymbol{\xi}_h \cdot \mathbf{u}_y), \tag{81k} \\ \delta z_{Hh} = G_H(\pi \boldsymbol{\xi}_h \cdot \mathbf{u}_y) \mu \mathbf{X}_h \cdot \mathbf{u}_y. \tag{81l} \end{array} \right.$$

The initial conditions are given by

$$\left\{ \begin{array}{l} Q_h^0 = \pi Q_h^{1/2} = P_h^0 = \pi P_h^{1/2} = 0, \\ \theta_h^0 = \pi \theta_h^{1/2} = \theta_0, \\ T_{h,1}^0 = \pi T_{h,1}^{1/2} = T_{h,2}^0 = \pi T_{h,2}^{1/2} = 0, \\ z_h^0 = \sqrt{c}, \\ \boldsymbol{\xi}_h^0 = \pi \boldsymbol{\xi}_h^{1/2} = L \begin{pmatrix} \cos(\theta_0) \\ \sin(\theta_0) \end{pmatrix} - H \begin{pmatrix} \sin(\theta_0) \\ -\cos(\theta_0) \end{pmatrix}, \\ \mathbf{X}_h^0 = 0, \\ z_H^0 = \sqrt{cH} \end{array} \right. \tag{82}$$

and with  $\pi \mathbf{u}_r = \begin{pmatrix} \cos(\pi\theta) \\ \sin(\pi\theta) \end{pmatrix}$  and  $\pi \mathbf{u}_\theta = \begin{pmatrix} \sin(\pi\theta) \\ -\cos(\pi\theta) \end{pmatrix}$ .

All the nonlinear arguments of the auxiliary functions  $\mathbb{G}_q$ ,  $\mathbb{G}_\theta$  and  $G_H$  are treated explicitly with the approximation  $\pi$ . So this scheme is linearly implicit and does not need any iterative procedure to be solved. The

drawback is that the matrix to invert changes at every iteration, but this problem can very often be limited with the use of special inversion formulas (see next Sect. 3.5).

Note that  $M_h V_h \in \mathbb{R}^{2n_h}$  and  $M_h V_h \cdot V_h \in \mathbb{R}$  are constant over time and can be pre-computed before the time iterations.

### 3.4.3. Discrete power balance

The scheme (81) reproduces a discrete analog of the continuous power balance (3.2).

**Theorem 3.9** (Discrete power balance of the scheme (81)). *The solution to the scheme (81) verifies*

$$\begin{cases} \delta \mathcal{E}_h = F_{h,Q}^{n+1/2} \cdot \mu P_h + F_{h,\theta}^{n+1/2} \mu T_{h,1}, & (83a) \\ \mathcal{E}_h^n = \frac{1}{2} M_h (P_h^n - V_h T_{h,1}^n) \cdot (P_h^n - V_h T_{h,1}^n) + \frac{1}{2} K_h Q_h^n \cdot Q_h^n + \frac{1}{2} (z_h^n)^2 + \frac{1}{2} (z_{Hh}^n)^2 \\ \quad + \frac{1}{2} m_H |\mathbf{X}_h^n|^2 + m_{Hg} \boldsymbol{\xi}_h^n \cdot \mathbf{u}_y. & (83b) \end{cases}$$

*Proof.* Take the inner product of (81d) with  $\mu P_h$ , multiply (81f) by  $\mu T_{h,1}$ , multiply (81i) by  $\mu \mathbf{X}_h$ , and sum these three contributions to get

$$\begin{aligned} & M_h \delta P_h \cdot \mu P_h + K_h \mu Q_h \cdot \mu P_h - \delta T_{h,1} M_h V_h \cdot \mu P_h + \mu z_h \mathbb{G}_q(\pi Q_h, \pi P_h, \pi \theta_h, \pi T_{h,1}, \pi T_{h,2}) \cdot \mu P_h \\ & + \mu T_{h,2} \mu T_{h,1} M_h V_h \cdot V_h - \mu T_{h,1} M_h V_h \cdot \delta P_h + \mu z_h \mathbb{G}_\theta(\pi Q_h, \pi P_h, \pi \theta_h, \pi T_{h,1}, \pi T_{h,2}) \mu T_{h,1} \\ & + m_H \delta \mathbf{X}_h \cdot \mu \mathbf{X}_h + m_{Hg} \mathbf{u}_y \cdot \mu \mathbf{X}_h + F_{\text{obs}} \mathbf{u}_y \cdot \mu \mathbf{X}_h \\ & = (\mathbf{F}_{\text{coupl}} \cdot \pi \mathbf{u}_\theta) \mu P_h \cdot I_h^{w(L)} + F_{h,Q}^{n+1/2} \cdot \mu P_h \\ & + \left( \pi Q_h \cdot I_h^{w(L)} - H \right) (\mathbf{F}_{\text{coupl}} \cdot \pi \mathbf{u}_r) \mu T_{h,1} - L (\mathbf{F}_{\text{coupl}} \cdot \pi \mathbf{u}_\theta) \mu T_{h,1} + F_{h,\theta}^{n+1/2} \mu T_{h,1} - \mathbf{F}_{\text{coupl}} \cdot \mu \mathbf{X}_h. \end{aligned} \quad (84)$$

The interior coupling force in the right-hand side vanishes thanks to equation (81j). The nonlinear terms simplify because of equation (81g):

$$\mu z_h \mathbb{G}_q(\pi Q_h, \pi P_h, \pi \theta_h, \pi T_{h,1}, \pi T_{h,2}) \cdot \mu P_h + \mu z_h \mathbb{G}_\theta(\pi Q_h, \pi P_h, \pi \theta_h, \pi T_{h,1}, \pi T_{h,2}) \mu T_{h,1} = \mu z_h \delta z_h, \quad (85)$$

and similarly for the head terms with equations (81k) and (81l):

$$F_{\text{obs}} \mathbf{u}_y \cdot \mu \mathbf{X}_h = \mu z_{Hh} G_H(\pi \boldsymbol{\xi}_h \cdot \mathbf{u}_y) \mu \mathbf{X}_h \cdot \mathbf{u}_y = \mu z_{Hh} \delta z_{Hh}. \quad (86)$$

After using the equations to substitute  $\delta$  and  $\mu$  when necessary, it remains:

$$\begin{aligned} & M_h \delta P_h \cdot \mu P_h - \delta T_{h,1} M_h V_h \cdot \mu P_h + \delta T_{h,1} \mu T_{h,1} M_h V_h \cdot V_h - \mu T_{h,1} M_h V_h \cdot \delta P_h + K_h \mu Q_h \cdot \mu P_h \\ & + \mu z_h \delta z_h + \mu z_{Hh} \delta z_{Hh} + m_H \delta \mathbf{X}_h \cdot \mu \mathbf{X}_h + m_{Hg} \mathbf{u}_y \cdot \delta \boldsymbol{\xi}_h = F_{h,Q}^{n+1/2} \cdot \mu P_h + F_{h,\theta}^{n+1/2} \mu T_{h,1}. \end{aligned} \quad (87)$$

The proof is completed after noticing that

$$\begin{aligned} & \frac{1}{2\Delta t} \left[ M_h \left( P_h^{n+1} - V_h T_{h,1}^{n+1} \right) \cdot \left( P_h^{n+1} - V_h T_{h,1}^{n+1} \right) - M_h \left( P_h^n - V_h T_{h,1}^n \right) \cdot \left( P_h^n - V_h T_{h,1}^n \right) \right] \\ & = M_h \delta P_h \cdot \mu P_h - \delta T_{h,1} M_h V_h \cdot \mu P_h + \delta T_{h,1} \mu T_{h,1} M_h V_h \cdot V_h - \mu T_{h,1} M_h V_h \cdot \delta P_h. \end{aligned} \quad (88)$$

□

**Remark 3.10.** The only term which is not necessarily positive is  $m_{Hg} \boldsymbol{\xi}_h^n \cdot \mathbf{u}_y$ , but it is only due to the definition of the origin of the Cartesian referential in which the potential energy due to gravity is computed. A positive constant can be added to this term to make sure it is positive without any loss of generalities.

TABLE 1. Values of the model parameters used in the simulations.

Shank parameters						
$L$ [m]	$S$ [m <sup>2</sup> ]	$\rho$ [kg/m <sup>3</sup> ]	$E$ [Pa]	$G$ [Pa]	$I$ [m <sup>4</sup> ]	$\kappa$ [-]
0.13	$6.31868 \times 10^{-5}$	560	$10.18 \times 10^9$	$0.64 \times 10^9$	$6.38999 \times 10^{-9}$	0.85

Head parameters					
$m_H$ [g]	$H$ [m]	$d_0$ [m]	$y_s$ [m]	$p$ [-]	$K$
12.09	0.025	0.027659	0.0565	1.8	$4 \times 10^8$

### 3.5. Solving strategy

Quadratized schemes can usually be solved by Sherman-Morrison-Woodbury formulas (see [30,34]) by eliminating auxiliary variables through Schur complements techniques. These methods avoid complete re-inversion of a new matrix at each time step, and instead allow the inverse to be updated by a low-rank perturbation. More precisely, the auxiliary variables are eliminated by the relation

$$\mu z = \frac{\Delta t}{2} \delta z + z^n. \quad (89)$$

Then the Lagrange multiplier  $\lambda_h$  and the coupling force  $\mathbf{F}_{\text{coupl}}$  should be eliminated, and finally the unknowns  $T_{h,1}^{n+1}$  and  $T_{h,2}^{n+1}$ . After that one would obtain only one equation to solve to compute  $P_h^{n+1}$  of the form

$$[A_h + U_h(t^n, t^{n-1})a_h {}^tU_h(t^n, t^{n-1})]\mu P_h = b(t^n, t^{n-1}), \quad (90)$$

with a right-hand side  $b$ ,  $A_h$  a constant matrix of size  $2n_h \times 2n_h$ ,  $a_h$  also constant of size  $k \times k$ , and  $U$  a changing matrix of size  $2n_h \times k$ . Then the Woodbury [34] inversion formula writes

$$[A_h + U_h(t^n, t^{n-1})a_h {}^tU_h(t^n, t^{n-1})]^{-1} = A_h^{-1} - A_h^{-1}U_h(a_h^{-1} + {}^tU_h A_h^{-1}U_h)^{-1} {}^tU_h A_h^{-1}. \quad (91)$$

The inverse  $A_h^{-1}$  is pre-computed once and for all, and if  $k$  is small enough the update only requires a cheap inversion of  $(a_h^{-1} + {}^tU_h A_h^{-1}U_h)^{-1}$  of size  $k \times k$  and a few matrix-vector products.

In the present case,  $k = 3$  and the computational cost is divided by about 3 when using this technique compared to a direct inversion of (81) in practical cases.

## 4. NUMERICAL RESULTS

This section first presents results for a flexible hammer alone that comes into contact with a rigid wall in order to demonstrate the good behaviour of the scheme proposed above. Secondly, in order to show its practical use for the numerical simulation of the piano, a simulation result with a coupling to a geometrically exact nonlinear string is presented. The C++ source code used for the following simulations is distributed under a GPLv3 licence, see [6].

### 4.1. Source input

For the simulations we use the parameters listed in Table 1 based on the hammer models of [7,32].

For the source term  $f_w$ , a  $C^\infty$  function in space and time is applied. It is displayed in Figure 3 and writes

$$f_w(x, t) = \begin{cases} A e^{\frac{1 - \frac{1}{1 - (\frac{x-x_0}{\sigma_x})^2}}}{1 - (\frac{x-x_0}{\sigma_x})^2}} e^{\frac{1 - \frac{1}{1 - (\frac{t-t_0}{\sigma_t})^2}}}{1 - (\frac{t-t_0}{\sigma_t})^2}} & \text{if } (x, t) \in [x_0 - \sigma_x, x_0 + \sigma_x] \times [t_0 - \sigma_t, t_0 + \sigma_t], \\ 0 & \text{otherwise.} \end{cases}$$

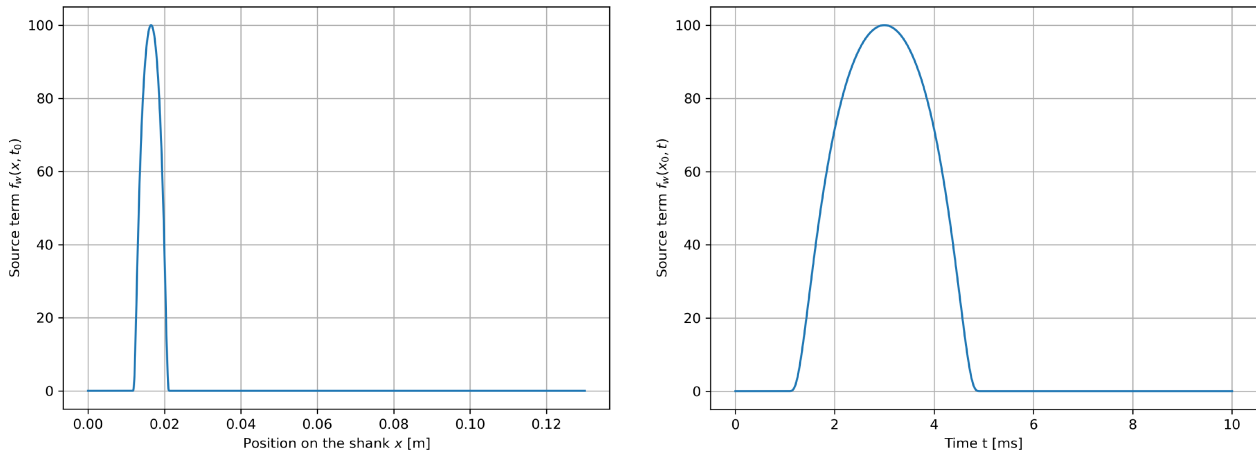


FIGURE 3. Source function  $f_w$  for fixed time (*left*) and fixed space (*right*).

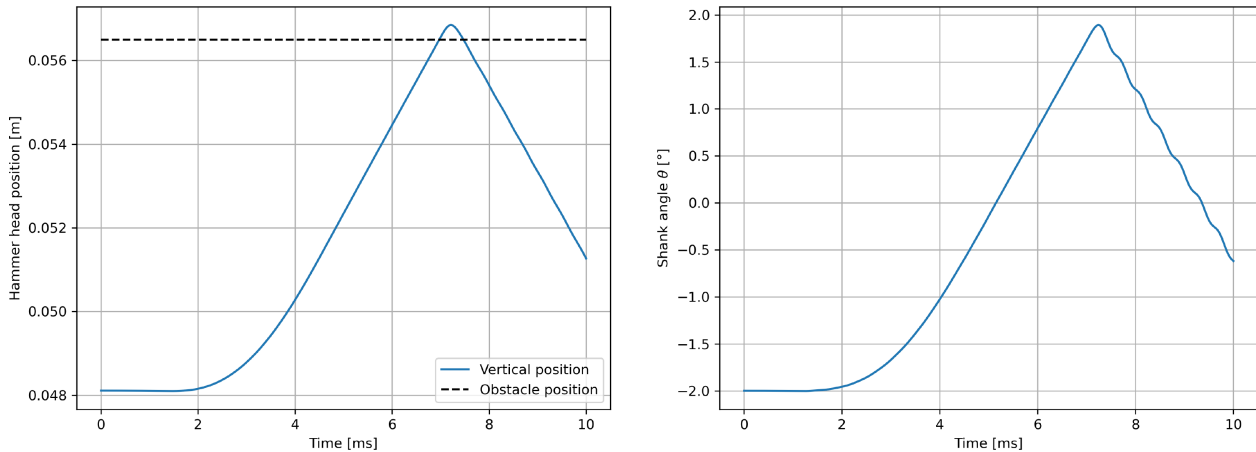


FIGURE 4. Evolution of the hammer head position (*left*) and shank angle (*right*).

with  $A = 100$ ,  $t_0 = 3$  ms,  $\sigma_t = 2$  ms,  $x_0 = 0.0165$  m and  $\sigma_x = 0.005$  m, meaning that the source starts at  $t = 1$  ms and ends at  $t = 5$  ms and is applied on the shank at the usual position of the hammer knuckle. The other source terms  $f_\varphi$  and  $f_\theta$  are set to zero in this simplified case, but would be non-zero with a force  $\mathbf{F}_{meca}$  coming from a real piano action (measured or simulated).

### 4.2. Solution

The following numerical results are computed with 49 elements of order 4 and with a time step  $\Delta t = 10^{-6}$ s. The auxiliary constants  $c$  and  $c_H$  are chosen equal to 1, and the initial angle of the shank is  $\theta = -2^\circ$ .

Figure 4 shows the motion of the hammer head perpendicularly to the obstacle. The hammer accelerates upwards between 0 and 7 ms, then makes contact with the obstacle between 7 and 7.5 ms. Then it changes direction and goes back downwards. The crushing of the hammer during the contact is clearly visible. On the right-hand side figure the angle  $\theta$  shows some oscillations after the contact occurred.

The deformations of the shank are visible on Figure 5. The application of the source is visible between 1 and 5 ms, and then the shank oscillates freely between 5 and 7 ms (the hammer is not submitted to any force except

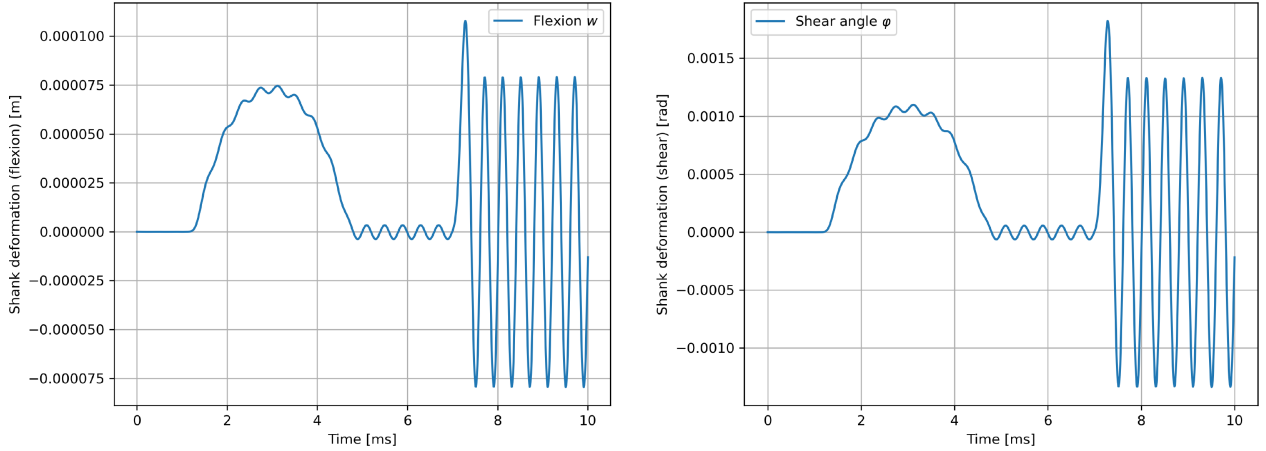


FIGURE 5. Evolution of the vibrations of the tip ( $x = L$ ) of the shank, flexion  $w(L, t)$  (left) and shear  $\varphi(L, t)$  (right).

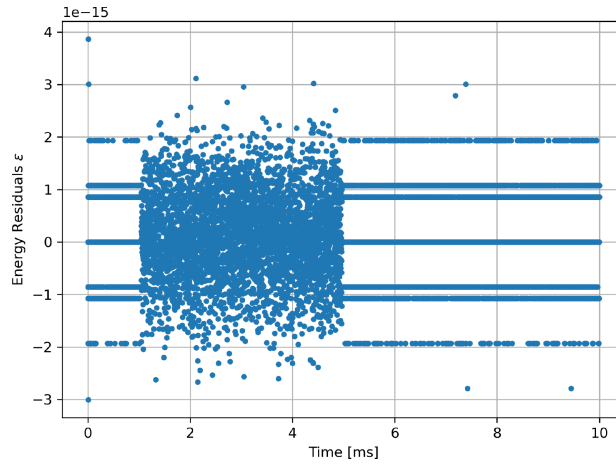


FIGURE 6. Evolution of the energy residual  $\varepsilon$  as defined in (93).

gravity). The contact with the obstacle occurs between 7 and 7.5 ms and the amplitude of the oscillations are greatly amplified.

### 4.3. Discrete power balance

The discrete energy is well preserved in the sense of Theorem 3.9. Let us introduce the energy residual  $\varepsilon$  as

$$\varepsilon = \frac{\mathcal{E}_h^{n+1} - \mathcal{E}_h^n}{\mathcal{E}_{\max}} - F_{h,Q}^{n+1/2} \cdot \frac{Q_h^{n+1} - Q_h^n}{\mathcal{E}_{\max}}. \quad (93)$$

The energy residual  $\varepsilon$  are multiples of the machine error on Figure 6, excepted during the application of the source which corresponds to the erratic part between 1 and 5 ms.

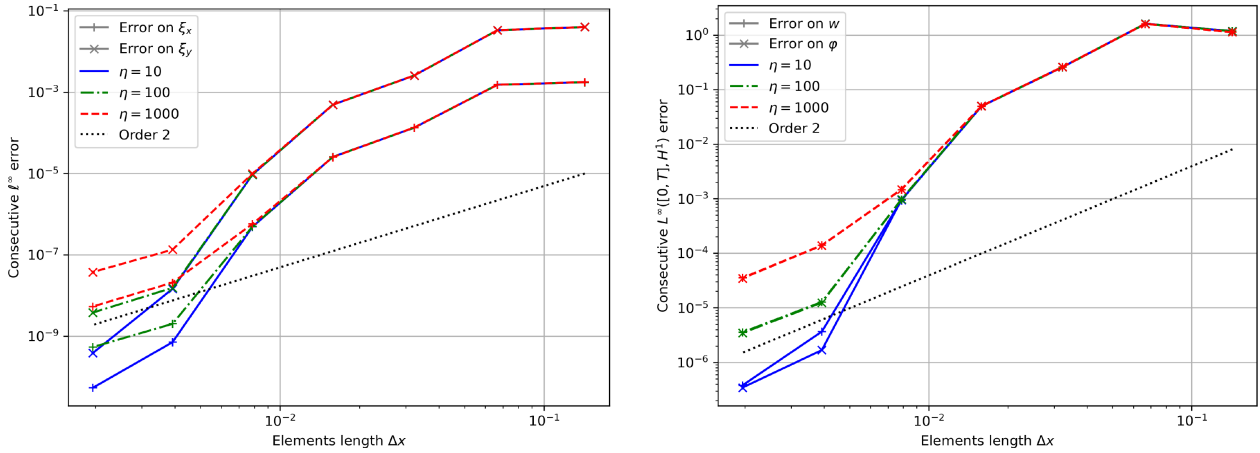


FIGURE 7. Space-Time convergence curves for different values of  $\eta$ : 10 in solid blue line, 100 in dashed green line, 1000 in dotted red line. *Left*: consecutive relative  $\ell^\infty$  in time error with respect to the spatial discretisation parameter  $\Delta x$  on the two components  $x$  (+ symbol) and  $y$  ( $\times$  symbol) of the variable  $\xi$ . *Right*: consecutive relative  $L^\infty([0, T]; H^1)$  error with respect to the spatial discretisation parameter  $\Delta x$  on the variables  $w$  (+ symbol) and  $\varphi$  ( $\times$  symbol).

#### 4.4. Computation times and convergence

The scheme (81) unconditionally satisfies the power balance, hence is expected to be unconditionally stable. To perform a space/time convergence analysis, we still introduce a parameter  $\eta$  acting as a fictive CFL ratio

$$\eta = \Delta t^2 \rho (M_h^{-1} K_h). \quad (94)$$

The convergence errors are computed consecutively between a solution computed with  $N_x$  elements and the refined solution with  $2N_x$  elements. They are compared on an interpolated regular grid of 100 points. The computed errors on the scalar unknowns are defined as

$$\forall (X, Y) \in \mathbb{R}^n \times \mathbb{R}^n, \quad E_{\ell^\infty}(X, Y) = \frac{\|X - Y\|_\infty}{\|Y\|_\infty} = \frac{\max_{i \in [1, n]} |x^i - y^i|}{\max_{i \in [1, n]} |y^i|}, \quad (95)$$

and the computed errors on the distributed unknowns are defined as

$$\forall (X_h^1, \dots, X_h^n, Y_h^1, \dots, Y_h^n) \in \mathcal{Q}_h^{2n}, \quad E_{L^\infty([0, T], H^1)}(X, Y) = \frac{\max_{i \in [1, n]} \|X_h^i - Y_h^i\|_{H^1}}{\max_{i \in [1, n]} \|Y_h^i\|_{H^1}}, \quad (96)$$

where for all  $X \in \mathcal{Q}_h$ ,

$$\|X\|_{H^1}^2 = \|X\|_{L^2}^2 + \|\nabla X\|_{L^2}^2. \quad (97)$$

Figure 7 shows space-time convergence curves for different values of  $\eta$ . The convergence rate after the pre-asymptotic regime is quadratic. However we were unable to go further in precision because of very long computation times.

Figure 8 plots the evolution of the errors with respect to the computation cost for different values of  $\eta$ . The computation costs are indicative and relative to the cheapest simulation.

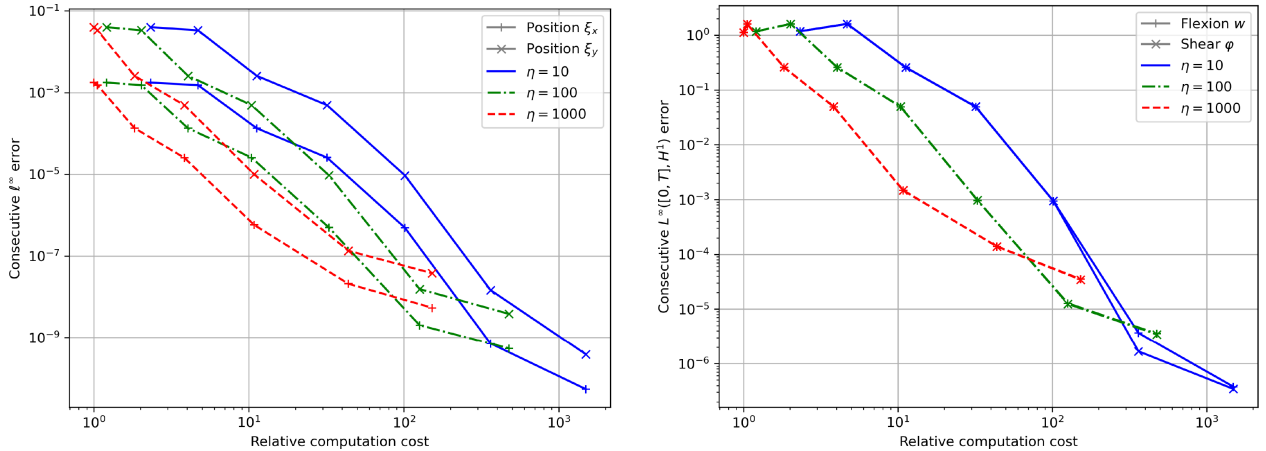


FIGURE 8. Error-Efficiency curves for different values of  $\eta$ : 10 in solid blue line, 100 in dashed green line, 1000 in dotted red line. *Left*: consecutive relative  $\ell^\infty$  in time error with respect to relative computation cost on the two components  $x$  (+ symbol) and  $y$  ( $\times$  symbol) of the variable  $\xi$ . *Right*: consecutive relative  $L^\infty([0, T]; H^1)$  error with respect to relative computation cost on the variables  $w$  (+ symbol) and  $\varphi$  ( $\times$  symbol).

TABLE 2. Values of the model parameters used for the string [8].

		String parameters						
$L$ [m]	$S$ [m <sup>2</sup> ]	$\rho$ [kg/m <sup>3</sup> ]	$T_0$ [N]	$E$ [Pa]	$G$ [Pa]	$I$ [m <sup>4</sup> ]	$\kappa$ [-]	
0.961	$8.6425 \times 10^{-7}$	7850	766	$2.02 \times 10^{11}$	$8 \times 10^{10}$	$5.9439 \times 10^{-14}$	0.85	

**Remark 4.1.** The fact that only one linear system must be solved at each time iteration induces a computational gain over the iterative gradient method proposed in [9], where the number of iteration per time step is not known in advance, and depends on the initial guess given by the user and on the time step. Note also that, if the time step is too large, the iterative method often fails (for two possible reasons: the nonlinear problem might not have a solution, and the initial guess might be too far away for the iterative algorithm to converge), which prevents from performing comparison tests. However, such a comparison has been performed for quadratized schemes applied to the geometrically exact string in Figure 8 of [5]. It shows that the quadratization yields a gain in accuracy of about a factor 10 for a given computation time.

#### 4.5. Coupling with a nonlinear string

To demonstrate the applicability of our method, we show in this paragraph a more complete example in which the flexible hammer comes into contact with a geometrically exact stiff nonlinear string (see [4] for more details). The physical parameters of this string are summarised in Table 2.

Such a string corresponds to a F3 note with fundamental frequency  $f_0 \approx 175$  Hz. The contact with the hammer head is distributed on a 2 centimeters zone, centered on a strike point  $x_s = L/8$ . To solve the nonlinear equations of the string, the phase-SAV discretization strategy is adopted along with high-order finite elements in space [4, 5] and coupled to the quadratisation technique applied to the flexible hammer shank in rotation presented above. The string is discretized with 49 elements of order 4 and the shank with 9 elements of order 2. The time step is chosen equal to  $10^{-6}$  s. The other shank parameters are the same as in the previous section. Dirichlet boundary conditions are enforced weakly for the string at  $x = L$  with two Lagrange multipliers,  $F^L$

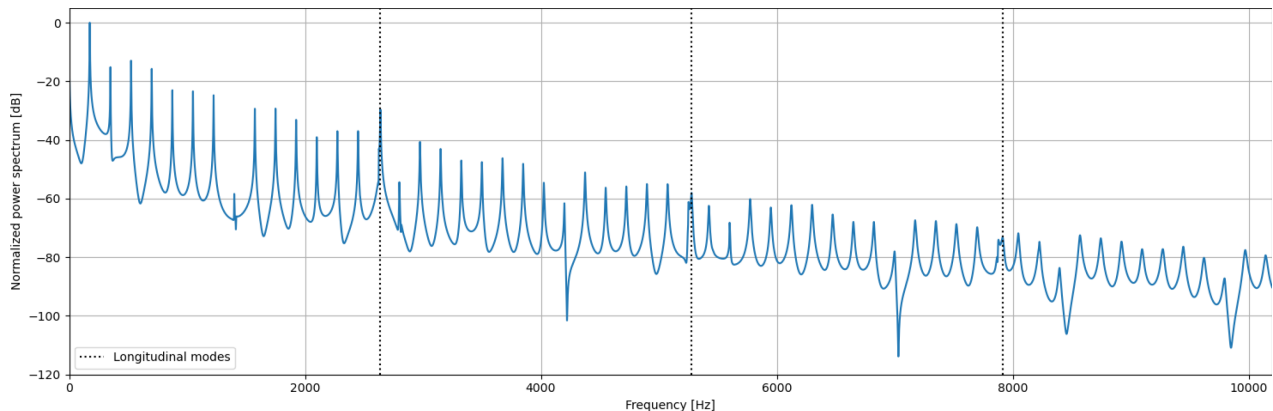


FIGURE 9. Normalized power spectrum of the Lagrange multipliers (Fourier transform of  $F^L + G^L$ ) at the end of the string with respect to the frequency. The harmonic frequencies of the longitudinal linearized wave are represented in dashed vertical lines.

for the transverse vibration and  $G^L$  for the longitudinal one. They represent the forces exerted by the string at this end point. On an algorithmic point of view, the coupling of the shank and the string requires to solve a linear system which must be updated at each time step.

In the absence of a soundboard, the sum  $F^L + G^L$  is a good “listening” signal because it is the force by which all the spectral content of the string is transmitted. The soundboard would mostly act as a filter on this force.

The power spectrum of  $F^L + G^L$  is represented on Figure 9. The influence of the strike point is very clearly visible: partials with ranks multiples of 8 are significantly reduced [1]. The longitudinal partials of the string are also clearly visible as they stand out from other transverse partials.

## 5. CONCLUSION AND PROSPECTS

This paper presents a quadratization method applicable for all energy nonlinearities, whether of potential or kinetic origin. A linearly implicit time-discretization scheme, formulated in the constrained phase space, which preserves a discrete power balance, has been given.

These general techniques were then applied to a rotating flexible piano hammer, which exhibits both kinetic and potential nonlinear energy terms. For this application, the scheme achieves a discrete power balance with no conditions on the discretization parameters, and converges in space/time with order 2.

In the case of the piano hammer, only the unknown  $\theta$  presents its second derivative  $\ddot{\theta}$  in the nonlinear function but the distributed unknown  $\ddot{q}$  does not appear. The proposed scheme deserves to be tested on a system exhibiting nonlinearity with a  $\ddot{q}$  sought in  $L^2$ , typically with discontinuous finite elements, in order to verify its correct convergence.

This method quadratizes all energy nonlinearities. The complete analysis of stability and convergence is an open problem that constitutes a perspective of this work, supported by preliminary numerical illustrations. Another interesting line of research would be to construct a similar quadratization technique for dissipative nonlinear terms (right-hand-side of Eq. (4)), leading to a linearly implicit scheme.

Finally, we mention that this scheme could be used to strike vibrating piano strings. Coupled with the work of [7] for the vibratory part (strings, soundboard, acoustic radiation), and with the work of [32] for the calculation of the input force  $\mathbf{F}_{\text{meca}}$  by a mechanical model, we would have a complete and efficient piano simulation tool that would allow us to study the influence of the pianist’s touch on the sound of his instrument.

## DATA AVAILABILITY STATEMENT

The C++ code used in this paper is available online under GPLv3 licence in a Gitlab repository: <https://gitlab.inria.fr/pianotouch/pianolib> [6].

## REFERENCES

- [1] A. Askenfelt and E.V. Jansson, From touch to string vibrations. III: string motion and spectra. *J. Acoust. Soc. Am.* **93** (1993) 2181–2196.
- [2] S. Bilbao, A. Torin and V. Chatziioannou, Numerical modeling of collisions in musical instruments. *Acta Acust. United Acust.* **101** (2015) 155–173.
- [3] J. Cai and J. Shen, Two classes of linearly implicit local energy-preserving approach for general multi-symplectic Hamiltonian PDEs. *J. Comput. Phys.* **401** (2020) 108975.
- [4] G. Castera, *Modélisation, analyse numérique et simulation de la propagation des ondes longitudinales dans le piano. Application à l'étude du toucher instrumental*. Ph.D. thesis, Université de Pau et des Pays de l'Adour (2023).
- [5] G. Castera and J. Chabassier, Numerical analysis of quadratized schemes. Application to the simulation of the nonlinear piano string. Technical Report RR-9516, Inria Bordeaux – Sud-Ouest (2023).
- [6] G. Castera and J. Chabassier, Pianolib, C++ toolbox for piano simulation (2024). <https://gitlab.inria.fr/pianotouch/pianolib>, ([hal-04571401](https://hal.archives-ouvertes.fr/hal-04571401)).
- [7] J. Chabassier, *Modélisation et simulation numérique d'un piano par modèles physiques*. Ph.D. thesis, École polytechnique (2012).
- [8] J. Chabassier and M. Duruffé, Physical parameters for piano modeling. Technical report (2012).
- [9] J. Chabassier and M. Duruffé, Energy based simulation of a Timoshenko beam in non-forced rotation. Influence of the piano hammer shank flexibility on the sound. *J. Sound Vib.* **333** (2014) 7198–7215.
- [10] J. Chabassier and S. Imperiale, Space/time convergence analysis of a class of conservative schemes for linear wave equations. *C. R. Math.* **355** (2017) 282–289.
- [11] J. Chabassier and P. Joly, Energy preserving schemes for nonlinear Hamiltonian systems of wave equations: application to the vibrating piano string. *Comput. Methods Appl. Mech. Eng.* **199** (2010) 2779–2795.
- [12] V. Chatziioannou and M. Van Walstijn, Energy conserving schemes for the simulation of musical instrument contact dynamics. *J. Sound Vib.* **339** (2015) 262–279.
- [13] M. Ducceschi and S. Bilbao, Non-iterative, conservative schemes for geometrically exact nonlinear string vibration, in Proceedings of the 23rd International Congress on Acoustics. Deutsche Gesellschaft für Akustik (2019).
- [14] M. Ducceschi and S. Bilbao, Simulation of the geometrically exact nonlinear string via energy quadratisation. *J. Sound Vib.* **534** (2022) 117021.
- [15] M. Ducceschi, S. Bilbao and C.J. Webb, Real-time simulation of the struck piano string with geometrically exact nonlinearity via a scalar quadratic energy method, in Proceedings of the 10th European Nonlinear Dynamics Conference (2022).
- [16] O. Gonzalez, Exact energy and momentum conserving algorithms for general models in nonlinear elasticity. *Comput. Methods Appl. Mech. Eng.* **190** (2000) 1763–1783.
- [17] M. He and P. Sun, Energy-preserving finite element methods for a class of nonlinear wave equations. *Appl. Numer. Math.* **157** (2020) 446–469.
- [18] A. Izabdakhsh, J. McPhee and S. Birkett, Dynamic modeling and experimental testing of a piano action mechanism with a flexible hammer shank. *J. Comput. Nonlinear Dyn.* **3** (2008) 031004.
- [19] C. Jiang, W. Cai and Y. Wang, A linearly implicit and local energy-preserving scheme for the sine-Gordon equation based on the invariant energy quadratization approach. *J. Sci. Comput.* **80** (2019) 1629–1655.
- [20] C. Jiang, Y. Wang and Y. Gong, Explicit high-order energy-preserving methods for general Hamiltonian partial differential equations. *J. Comput. Appl. Math.* **388** (2021) 113298.
- [21] P. Joly, Variational methods for time-dependent wave propagation problems, in Topics in Computational Wave Propagation: Direct and Inverse Problems. Springer Berlin Heidelberg, Berlin, Heidelberg (2003) 201–264.
- [22] D. Li and W. Sun, Linearly implicit and high-order energy-conserving schemes for nonlinear wave equations. *J. Sci. Comput.* **83** (2020) 1–17.
- [23] L. Lin, Z. Yang and S. Dong, Numerical approximation of incompressible Navier-Stokes equations based on an auxiliary energy variable. *J. Comput. Phys.* **388** (2019) 1–22.

- [24] S. Lin, W. Shu and W. Yongxin, The well-posedness and regularity of a rotating blades equation. *Electron. Res. Arch.* **28** (2020) 691–719.
- [25] Z. Liu and X. Li, The exponential scalar auxiliary variable (E-SAV) approach for phase field models and its explicit computing. *SIAM J. Sci. Comput.* **42** (2020) B630–B655.
- [26] Z. Liu and X. Li, Step-by-step solving schemes based on scalar auxiliary variable and invariant energy quadratization approaches for gradient flows, in *Numerical Algorithms*. Springer (2022) 1–22.
- [27] M.A. Rincon and N.P. Quintino, Numerical analysis and simulation for a nonlinear wave equation. *J. Comput. Appl. Math.* **296** (2016) 247–264.
- [28] J. Shen and X. Yang, Numerical approximations of Allen-Cahn and Cahn-Hilliard equations. *Discrete Contin. Dyn. Syst.* **28** (2010) 1669–1691.
- [29] J. Shen, J. Xu and J. Yang, A new class of efficient and robust energy stable schemes for gradient flows. *SIAM Rev.* **61** (2019) 474–506.
- [30] J. Sherman and W.J. Morrison, Adjustment of an inverse matrix corresponding to a change in one element of a given matrix. *Ann. Math. Statist.* **21** (1950) 124–127.
- [31] A. Stulov, Experimental and theoretical studies of piano hammer, in *Proceedings of the Stockholm Music Acoustics Conference*. Stockholm, Sweden Vol. 485 (2003).
- [32] S. Timmermans, *Haptic key based on a real-time multibody model of a piano action*. Ph.D. thesis, Université catholique de Louvain (2021).
- [33] C.P. Vyasarayani, S. Birkett and J. McPhee, Modeling the dynamics of a compliant piano action mechanism impacting an elastic stiff string. *J. Acoust. Soc. Am.* **125** (2009) 4034–4042.
- [34] M.A. Woodbury, *Inverting Modified Matrices*. Statistical Research Group (1950).
- [35] X. Yang, Linear, first and second-order, unconditionally energy stable numerical schemes for the phase field model of homopolymer blends. *J. Comput. Phys.* **327** (2016) 294–316.
- [36] J. Zhao, Q. Wang and X. Yang, Numerical approximations for a phase field dendritic crystal growth model based on the invariant energy quadratization approach. *Int. J. Numer. Methods Eng.* **110** (2017) 279–300.



**Please help to maintain this journal in open access!**

This journal is currently published in open access under the Subscribe to Open model (S2O). We are thankful to our subscribers and supporters for making it possible to publish this journal in open access in the current year, free of charge for authors and readers.

Check with your library that it subscribes to the journal, or consider making a personal donation to the S2O programme by contacting [subscribers@edpsciences.org](mailto:subscribers@edpsciences.org).

More information, including a list of supporters and financial transparency reports, is available at <https://edpsciences.org/en/subscribe-to-open-s2o>.